PHILOSOPHICAL TRANSACTIONS A

royalsocietypublishing.org/journal/rsta

Review

Cite this article: Halvey AK, Macdonald B, Dhyani A, Tuteja A. 2019 Design of surfaces for controlling hard and soft fouling. *Phil. Trans. R. Soc. A* **377**: 20180266.
http://dx.doi.org/10.1098/rsta.2018.0266

Accepted: 12 October 2018

One contribution of 14 to a theme issue 'Bioinspired materials and surfaces for green science and technology'.

Subject Areas:
materials science

Keywords:
solid fouling, low adhesion, easy clean surfaces, elastic modulus, surface chemistry, coatings

Author for correspondence:
Anish Tuteja
e-mail: atuteja@umich.edu

Design of surfaces for controlling hard and soft fouling

Alex Kate Halvey[1,2], Brian Macdonald[1,2], Abhishek Dhyani[2,3] and Anish Tuteja[1,2,3,4]

[1]Department of Materials Science and Engineering, [2]BioInterfaces Institute, [3]Macromolecular Science and Engineering, and [4]Department of Chemical Engineering, University of Michigan, Ann Arbor, MI 48109, USA

AT, 0000-0002-2383-4572

In this review, we present a framework to guide the design of surfaces which are resistant to solid fouling, based on the modulus and length scale of the fouling material. Solid fouling is defined as the undesired attachment of solid contaminants including ice, clathrates, waxes, inorganic scale, polymers, proteins, dust and biological materials. We first provide an overview of the surface design approaches typically applied across the scope of solid fouling and explain how these disparate research efforts can be united to an extent under a single framework. We discuss how the elastic modulus and the operating length scale of a foulant determine its ability or inability to elastically deform surfaces. When surface deformation occurs, minimization of the substrate elastic modulus is critical for the facile de-bonding of a solid contaminant. Foulants with low modulus or small deposition sizes cannot deform an elastic bulk material and instead de-bond more readily from surfaces with chemistries that minimize their interfacial free energy or induce a particular repellant interaction with the foulant. Overall, we review reported surface design strategies for the reduction in solid fouling, and provide perspective regarding how our framework, together with the modulus and length scale of a foulant, can guide future antifouling surface designs.

This article is part of the theme issue 'Bioinspired materials and surfaces for green science and technology'.

THE ROYAL SOCIETY PUBLISHING

1. Introduction

The undesired adhesion of solid contaminants to a surface, particularly when the adhering material damages the desired properties of that surface, can be labelled as solid fouling. This broad area includes the surface adhesion of a diverse array of contaminants such as ice, clathrate hydrates of natural gases, wax, inorganic scale deposits, polymers in solution, proteins, dust and dirt, as well as a wide range of biofouling materials. Examples of the industrial problems caused by these materials include the attachment of marine organisms to ship hulls [1,2], icing of power lines and airplanes [3–5], deposition of asphaltenes and wax on systems in petroleum processing [6,7] and biofilm growth on medical devices [8,9]. It is therefore essential to either prevent the attachment and continued deposition of these solids or to facilitate their easy removal from critical surfaces.

Solid fouling materials vary widely in composition and chemical structure, as well as in their physical properties and modes of deposition. Many surfaces have been fabricated to resist the adhesion of these materials; however, research efforts have traditionally focused on only a single type of solid foulant when designing a surface. Therefore, an effort to establish a classification methodology for different solid foulants, particularly one which guides the design of antifouling surfaces, can be quite useful.

(a) Surface design strategies

Surface design approaches which have been shown to lower solid adhesion can be divided simplistically into three categories. The first, we will refer to as chemical functionalization. This strategy involves selecting or creating a surface chemistry which either lowers the substrate surface energy or allows the surface to interact in a particular way with the fouling material. Minimizing the energy of a surface reduces the strength of any potential adhesive interaction between the surface and a fouling material, known as the work of adhesion, W_a. The contribution of the interfacial free energy of a surface (γ_{s_1v}) to the work of adhesion is commonly represented by the equation $W_a = \gamma_{s_1v} + \gamma_{s_2v} - \gamma_{s_1s_2}$, where γ_{s_1v} and $\gamma_{s_1s_2}$ are the interfacial free energy for the foulant and the foulant–substrate interface, respectively [10,11]. Surfaces designed with this approach commonly use silicones or fluorinated polymers, which are among the lowest surface energy materials [12]. Beyond interfacial energy considerations, surface chemistries which interact specifically with a fouling material vary more widely, from zwitterionic polymer surfaces designed to repel biofilms and proteins [13–16], to conductive films for the repulsion of dirt and dust [17,18]. Common drawbacks of designing a surface based on chemical functionalization involve the lower attainable limit of surface energy and the complexity of achieving particular desired interactions.

The next design approach which can be used to limit solid fouling is tuning the physical properties of the surface, specifically its elastic modulus. In the case of a rigid material adhered to an elastic surface, the strength of that adhesive bond is proportional to both the work of adhesion and the elastic modulus, E, of the surface material by the relation $\sigma \propto \sqrt{W_a E/t}$, where t is the film thickness [19–21]. The rationale for this is that the total energy of a surface consists of both its elastic strain energy (a proportional function of modulus) and its interfacial free energy [19,21]. When the de-bonding of a contaminant from a surface involves the macro-scale deformation of the surface, as in a rigid material de-bonding from an elastic surface, this elastic strain can significantly increase the overall surface energy. Minimizing the elastic strain energy of the surface by reducing its modulus lowers the equilibrium barrier for fracture of the adhesive interface [21]. Therefore, by lowering the modulus of the surface material, the adhesion of solid fouling materials can be reduced dramatically. In fact, while the interfacial free energy difference between smooth surfaces of a high energy metal such as iron ($2.4\,\mathrm{J\,m^{-2}}$) [22] and the lowest energy material $C_{20}F_{42}$ ($0.0067\,\mathrm{J\,m^{-2}}$) [23] is only a factor of 100, the modulus between a hard and soft surface can vary over as many as 5 orders of magnitude [24,25]. Thus, when bulk deformation occurs,

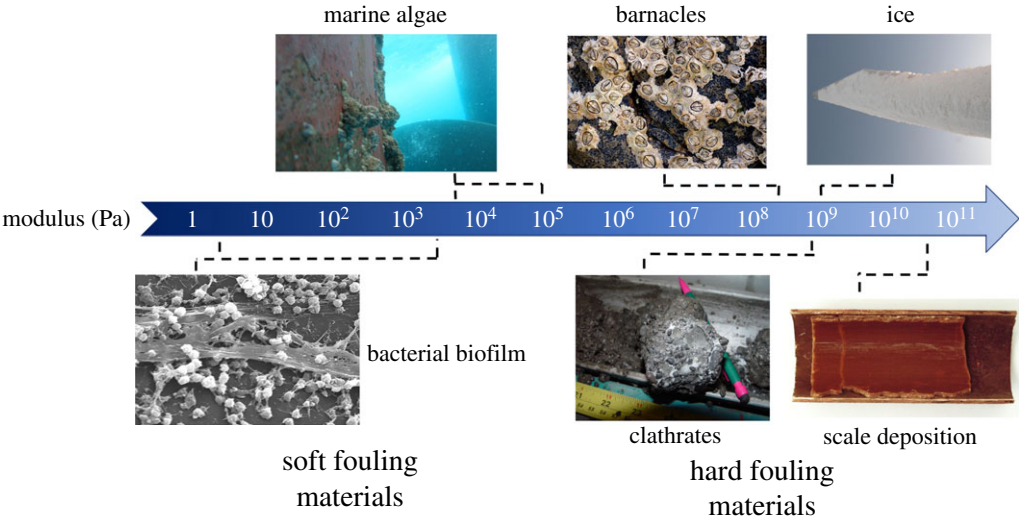

Figure 1. Fouling materials classified on the basis of modulus. Estimated values of modulus for: soft fouling materials such as bacterial biofilm on a catheter tube [30–32] (obtained from CDC Public Health Image Library under public domain) and marine algae adhered to a ship hull [33], along with hard fouling materials like barnacles [34] (image reproduced with permission from [35], licensed under https://creativecommons.org/licenses/by/4.0/), clathrates in petroleum pipelines [36] (image reproduced from www.usgs.gov under public domain), ice on a wind turbine blade [37] reproduced from [38] (with licence under https://creativecommons.org/licenses/by-nc-sa/3.0/) and inorganic scale deposited in a pipe carrying cooling water (licensed under https://creativecommons.org/licenses/by-sa/3.0/deed.en).

reduction in the surface modulus can have a more significant effect on foulant adhesion than the intrinsic work of adhesion of the surface, which is controlled by chemical functionalization. This approach raises one primary concern: the durability of low-modulus surface materials.

A final approach for surface design is control over surface microtexture. While textural approaches are a critical component of designing for the reduction in liquid fouling [26], in the case of solid fouling, microtexture is typically detrimental as it increases the adhesive/interfacial contact area or creates the potential for an interlocking interface across which de-bonding is significantly hindered [11,27–29]. Some niche applications using textured surfaces will be mentioned where relevant in this review, but overall, the approach is considered to be outside of the design guide proposed.

(b) Influence of foulant material properties

With these key design approaches defined, the question becomes how can the properties of a fouling material be used to determine which is the most effective approach towards antifouling surface design. As was just described, the mechanism for a solid to de-bond from a low-modulus surface involves the deformation of the surface by the fouling material when an external force is applied [19–21]. This deformation increases the elastic strain energy of the surface, which is limited by the modulus of its material [19,21]. However, when considering a broad list of potential foulants, it becomes clear that only foulants with sufficiently high intrinsic modulus will be able to cause the deformation of a plausible range of surface materials and de-bond via this mechanism. In these cases, the minimization of the elastic modulus of a surface will have a significant, and often dominating, effect on foulant adhesion. Therefore, it is apparent that the rigidity of the fouling material, and specifically, its modulus in comparison to potential surface moduli, is critical in directing low adhesion surface design. By categorizing fouling materials according to their

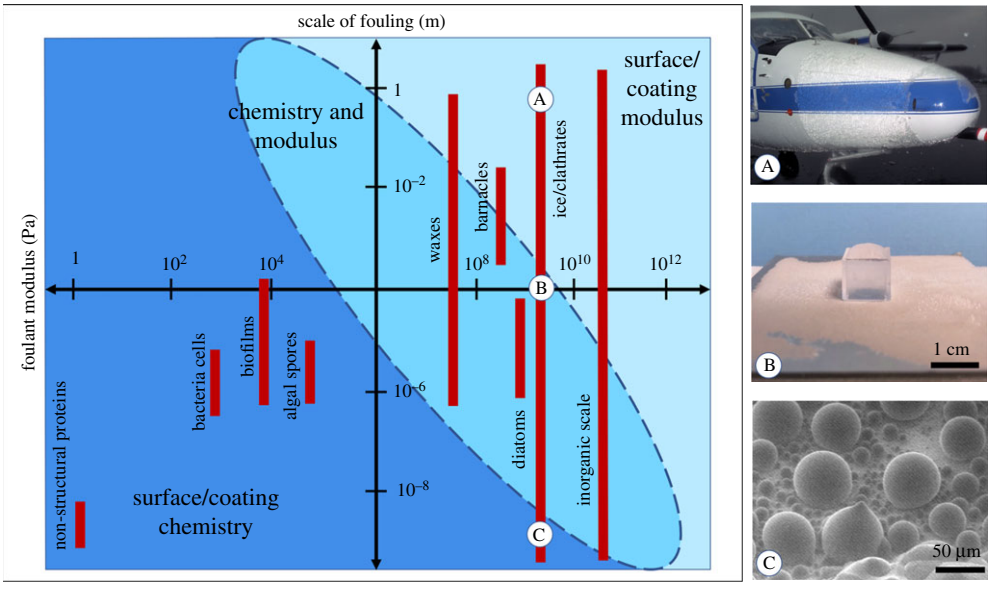

Figure 2. Low solid adhesion surface design guide, which categorizes fouling materials according to their length scale. Fouling length scales are indicated for bacterial cells [41], biofilm thickness [30,42], algal spores [43,44], diatoms [45], barnacles, wax [46] and ice [47–49]. Elastic modulus values for bacterial cells [50], biofilms [30–32], algal spores [33], diatoms [45], barnacles [34], wax [51,52], ice [37,53], clathrates [36,54] and inorganic scale [55,56] are also provided in order to indicate whether the effects of surface chemistry or surface elastic modulus will be most potent in minimizing the fouling of that material. Subset images A, B and C illustrate typical micro-, meso- and macro-scale ice fouling, respectively. Subset image A is an image provided by NASA, and is in the public domain. Subset image B was taken by the authors. Subset image C is adapted with permissions from [57], copyright © 2013 American Chemical Society.

elastic modulus, a general guide can be set which allows a researcher to predict the relative impact of chemical versus mechanical factors upon their surface design. This is illustrated in figure 1.

Although the straightforward simplicity of this division between hard and soft foulants is appealing, many surface design approaches do not fit this trend. Examples of this include surfaces designed to repel dry dirt or ice crystal nucleates, which rely on chemical approaches despite the high modulus of the typical components of soil and ice [17,18,39,40]. Clearly, the initial guide in figure 1 is insufficient to capture the scope of solid fouling. In revisiting the criteria for surface modulus-based design, it is evident that not only must the fouling material have adequate intrinsic modulus, but it must be of sufficient size in order to deform the bulk of the surface and bring elastic strain energy into consideration. With this in mind, an extra dimension needs to be added to our guide to account for the length scale of the fouling phenomena. A key example of this scale variation in a fouling material is ice, which can range from centimetres thick sheets with adhesion areas of square metres, to microscopic nucleation sites. Additionally, it is important to note that even for large, high modulus fouling materials, some reduction in adhesion due to the chemical functionalization of the surface can be obtained, as is indicated in the discussion above. What primarily varies across the scope of this design guide is the ability of a fouling material to deform a surface during de-bonding and thus bring elastic strain energy effects into consideration. The larger the degree of deformation of the surface, the more its elastic strain energy will contribute to the equilibrium barrier for fracture of the interface [21]. In these cases, the reduction in the surface modulus will have a dominant effect on minimizing the adhesion strength of the foulant, because the surface modulus can be tuned over many more orders of magnitude than the work of adhesion, which is controlled by chemical functionalization. For foulant materials of moderate modulus or length scale which cause only minor deformation of

most elastic surfaces during de-bonding, chemical functionalization and reduction in surface modulus have competing effects on foulant adhesion. The enhanced version of our guide, presented in figure 2, indicates which surface design approach, chemical functionalization or low-modulus substrate, will have a dominant effect in reducing solid adhesion. The delineations between the regions in this guide are estimated based on the predicted ability of foulants at each modulus and length scale to deform a range of elastic bulk materials. This design guide accounts for fouling from materials of moderate modulus or length scale where both strategies can be effective.

The remainder of this review is dedicated to an overview of a myriad of surfaces which have been designed to limit fouling from a wide range of contaminating solids. Discussion centres around the ways these designer surfaces fit into the framework presented in figure 2, as well as how this framework can guide the future of low adhesion surface design.

2. Ice fouling

One of the most significant examples of solid fouling that affects both commercial and residential activities is the unwanted accumulation of ice on surfaces. From nucleates of frost to sheets of solid glaze [58], ice contamination poses an expensive problem for many major industries. Common applications where ice is a challenge include airplane wings [3,4,59] and power lines [5,60], as well as locks and dams [61] and other mechanical components. Ice fouling also impacts renewable energy technology, impeding the function of solar panels [62] and wind turbines [63]. While a myriad of low ice adhesion (τ_{ice}) surface designs are proposed in the literature, the primary methods of combatting ice accumulation in industry still involve active deicing. Surface heating, by hot air or electrothermal pulses [4,63], is a common approach, but is extremely energy intensive. Similarly, mechanical shock or vibrations require both energy input and consistent surface monitoring [5]. Particularly for airplanes, organic liquids with low freezing temperatures are routinely sprayed onto surfaces to remove accumulated ice, which requires significant treatment time for a short-term solution [59]. These cases of ice fouling, combined with currently inadequate solutions, demand the development of passive, low ice adhesion surfaces which are durable enough to survive under relatively harsh environmental conditions.

In the context of solid fouling materials addressed in this review, ice has a very high innate material modulus, on the order of 1 GPa [37,53]. However, when placing low adhesion surface designs within the framework of figure 2, it is equally critical to note the exceptionally broad length scale over which ice can act as a foulant. The critical radius for an ice nucleus to become stable and grow is reported by multiple groups to be in the single nanometre range [47–49], while bulk ice can easily accumulate on industrial equipment in sheets, which are metres long and inches thick.

(a) Nucleation prevention

Beginning at the bottom of the length scale, many groups have worked to develop surfaces which delay or prevent the nucleation of ice. The most commonly attempted method in this regard has been the fabrication of superhydrophobic surfaces (SHP). Through a combination of low surface energy and microtexture [64], SHP surfaces support water above entrapped pockets of air (known as the Cassie–Baxter state) [65]. The low surface energy, minimal effective surface area and thermal insulation from entrapped air for an SHP surface in the Cassie–Baxter state is desirable to minimize opportunities for heterogenous ice nucleation. SHPs have displayed the ability to retard ice formation from saturated vapour onto a surface held at −8 to −10°C [66–69]. However, such surfaces were minimally effective at −23°C [66]. One nanotextured SHP designed by Jung *et al.* [49] was able to generate a 25 h freezing delay at −21°C. However, frost was eventually able to form on all surfaces under freezing conditions. Along with delaying frost formation, the ability of SHPs to bounce or roll water droplets off a surface [70] has led to experimentation and modelling on their capacity to repel freezing rain and condensate before it can nucleate [71]. It

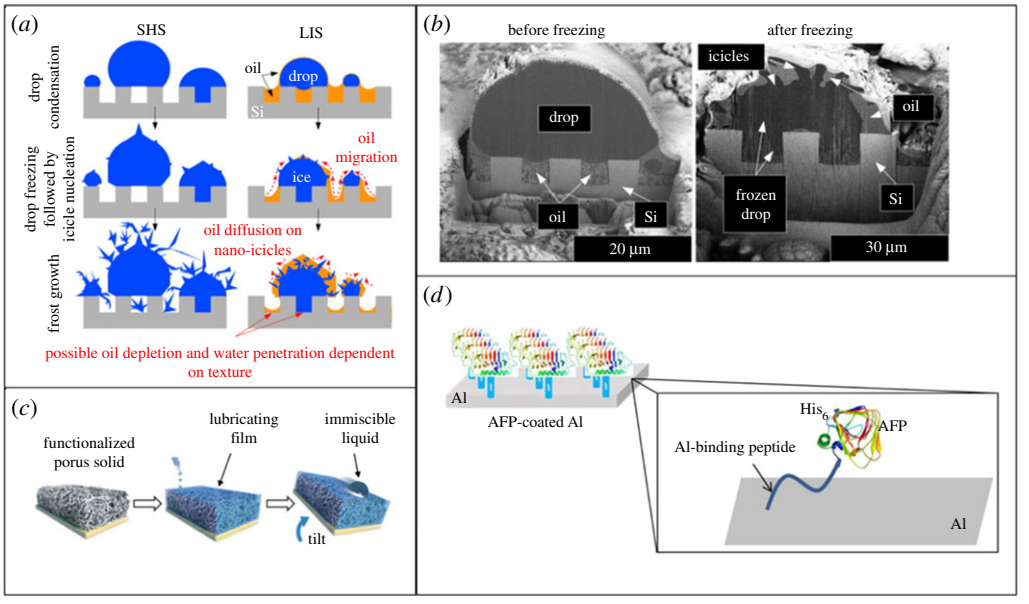

Figure 3. (*a*) The mechanism of ice nucleation via drop condensation and freezing on superhydrophobic surfaces and SLIPS-based surfaces. The images demonstrate the texture permeation for superhydrophobic surfaces during frost formation, and lubricant wicking from SLIPS-based surfaces. (*b*) Cryo-FIB/SEM images of a water droplet before and after freezing on oil impregnated silicon microposts (*a*,*b*) reprinted with permission from [57] Copyright © 2013 American Chemical Society. (*c*) Standard fabrication steps for a SLIPS-based lubricated coating; (*c*) adapted from [79] with permission. (*d*) Schematic diagram of AFP functionalized aluminium (adapted from [80] with permission from http://creativecommons.org/licenses/by/4.0/).

was determined by Bahadur *et al.* [71] that pinning and nucleation would occur before a falling droplet bounced off from an SHP surface at −20°C or below. Multiple groups have, however, reported that the application of sufficient pressure (including Laplace pressure) or exposure to small droplets (i.e. initial condensation) can instigate a transition from the Cassie–Baxter state to the Wenzel state where the contacting liquid displaces all the air present and fully wets the surface [48,70,72–78]. Critical issues with SHPs arise when ice or condensation is able to penetrate the surface texture (figure 3*a*). Such complete wetting leads to more rapid heterogenous nucleation due to an increase in effective surface area, as well as to the subsequent high adhesion of bulk ice which can interlock mechanically with the texture [27,72,76,81]. Lastly, the highly textured surfaces of SHP surfaces are subject to damage from mechanical abrasion, which increases the presented surface area for nucleation and limits the SHP surfaces' ability to delay ice deposition [72,82]. Ultimately, surface design has shifted away from the SHP approach under the realization that anti-icing designs must optimize the surface wettability while minimizing roughness [49].

Multiple chemical approaches have also been taken to limit ice nucleation onto a surface by engineering a particular interaction between the surface and ice nucleates. The grafting of antifreeze proteins (AFPs), found in organisms with the ability to survive in subzero conditions, has been shown to delay or prevent frost formation on aluminium and glass surfaces (figure 3*d*) [80,83]. Wong *et al.* [79] pioneered another novel approach to frost prevention: slippery liquid-infused porous surfaces or SLIPS. This approach is reliant on the inability of ice to nucleate on the molecularly smooth surface presented by an imbibed lubricant (figure 3*c*). Surfaces designed with this approach include a porous matrix that is functionalized in order to interact strongly with an infused liquid lubricant [79,84]. Within the framework of this review, lubricated surfaces are not considered as ultra-low-modulus solid surfaces. They behave as liquid surfaces which do not possess elastic strain energy when deformed, meaning that solid de-bonding from lubricated surfaces is not governed by the same mechanism as de-bonding from low-modulus elastic solids.

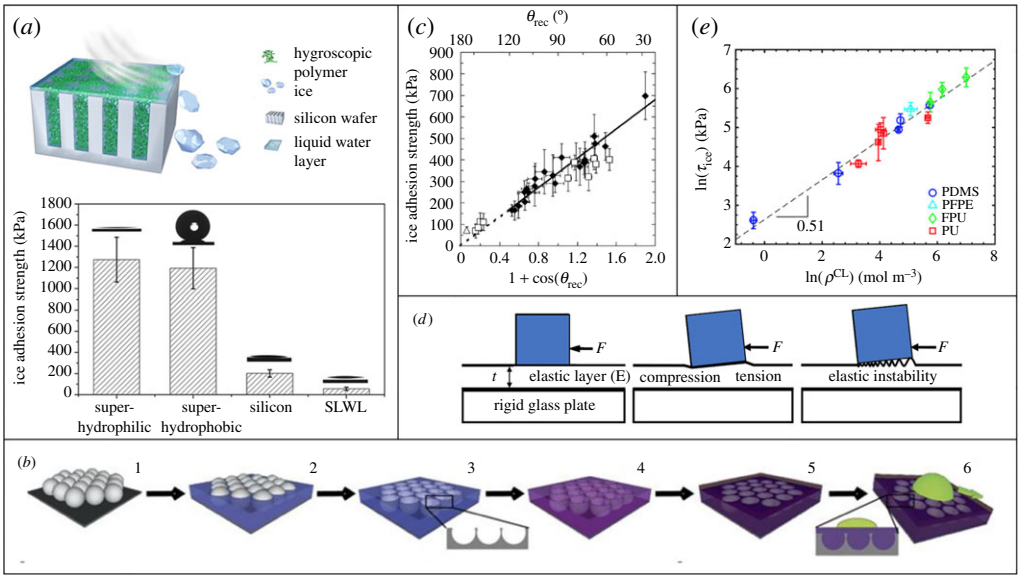

Figure 4. (*a*) A schematic illustrating a self-lubricating, water layer (SLWL) surface. The average ice adhesion strength values on four different surface types, superhydrophilic, superhydrophobic, silicon and SLWL are also shown (adapted from [82] Copyright © 2013 American Chemical Society). (*b*) Construction scheme for colloid templated SLIPS (reproduced with permission from [89]). (*c*) Average ice adhesion strengths measured at −10°C for bare steel and 21 different coatings plotted versus $1 + \cos(\theta_{rec})$—a variable that scales with the practical work of adhesion, and the receding contact angle θ_{rec} for water. (*c*) Adapted from [90] Copyright © 2010 American Chemical Society. (*d*) Schematic for a solid de-bonding from an elastic surface layer. (*d*) Adapted from [19] with permission. (*e*) Relationship between the elastomer cross-link density ρ^{CL} (a variable that is directly proportional to the shear modulus) and the ice adhesion strength (τ_{ice}) for coatings without interfacial slippage. (*e*) Adapted from [91] with permission from http://creativecommons.org/licenses/by/4.0/.

SLIPS-based surfaces have succeeded in delaying frost formation [85,86], allowing for the rapid defrosting of surfaces when heated to only 5°C [85], and lowering the nucleation temperature of water as far as −26°C [87]. The drawbacks of this design are the tendency of lubricant, including different perfluorinated oils and silicone oils, to wick out of the porous texture and onto the frost deposits occurring at non-lubricated sites (figure 3*a*,*b*), as well as the inability of porous texture asperities/lubricant to withstand mechanical damage [57,88].

In order to combat the issue of depleted lubricant, multiple groups have replaced the infused oil with tethered hygroscopic polymer chains, or simply tethered such polymers to the surface in the absence of porous texture. At low temperature, these chains deliquesce by absorbing water from condensation and swell to form a lubricating surface layer that melts incoming frost nucleates (figure 4*a*) [82,92–94]. In addition to being ecofriendly with no risk of leaching oils [82], these surfaces have been shown to be abrasion resistant [82], and to function at temperatures as low as −53°C [93]. A final approach to improving on the SLIPS design for antifrost surfaces was proposed by Sun *et al.* who fabricated a microporous surface impregnated with antifreeze and capped by an SHP layer. This design enabled their surface to repel the majority of condensation and falling droplets, while liquid or frost that penetrated the SHP texture caused the wicking of the antifreeze, which in turn caused their melting [95]. Although this surface is still vulnerable to eventual liquid depletion, the lubricant wicks out selectively, thereby lengthening its usable lifetime [95].

(b) Reduction in ice adhesion strength (τ_{ice})

Because of the many complexities and lack of success in preventing the adherence of ice nuclei and microscale deposits, especially over long periods of time, many research groups have instead

focused on the facile removal of bulk ice, ranging from approximately 1 cm cubes to large sheets. At an intermediate length scale, in accordance with the design framework given in figure 2, the effects of chemical functionalization and bulk modulus compete for dominance in surface design. With regard to chemical functionalization, a variety of methods have been used to obtain low interfacial energy coatings which inhibit hydrogen bonding with the forming ice. Petrenko & Peng [96] used a variety of self-assembled monolayers (SAMs) with a range of surface energies to demonstrate that the shear adhesion of ice scales with the work of adhesion. Meuler *et al*. [90] arrived at a similar conclusion by studying polymeric coatings filled with varying amounts of fluorinated polyhedral oligomeric silsesquioxane, a low-surface-energy additive (figure 4*c*). Zou *et al.* and Sojoudi *et al.* also confirmed this result using chemical vapour deposition (PECVD) of fluorinated and non-fluorinated components [97,98]. Fluorinated sol gels, and annealed silicone and fluorine containing block copolymers are among other coating types which demonstrate the utility of lowering solid surface energy to lower ice adhesion [99,100]. While these results are encouraging, the theoretical lower limit of τ_{ice} on a smooth, non-elastic, low-energy surface is only approximately 150 kPa [91]. Therefore, additional strategies are needed to fabricate low τ_{ice} surfaces.

One design approach is to capitalize on the mobile interface enabled by SLIPS surfaces, which were previously discussed in the context of ice nucleation. Many SLIPS surfaces have demonstrated low τ_{ice} [85,86,88,101], down to 15 kPa [85]. However, such surfaces are still afflicted by the tendency of the lubricant to leach out of the surface, and of the asperities of the porous matrix to sustain mechanical damage. Multiple modifications to SLIPS surfaces have been adapted in order to improve ice adhesion performance. Once again, surfaces containing hygroscopic polymers have been presented as an alternate method of generating a lubricated surface, and have been successful in reducing τ_{ice} to as low as 20 kPa (figure 4*a*) [82,92,93]. Vogel *et al.* [89] demonstrated ice adhesion values of only $\tau_{ice} = 10$ kPa by using colloidal templating to generate closed-cell silica microstructures for SLIPS with tunable porosity, improved containment of lubricant and superior mechanical durability (figure 4*b*). Yin *et al.* [81] adopted a similar fabrication methodology, with the addition of Fe_3O_4 nanoparticles for photoresponsive thermogenesis, to enable rapid, low-energy surface heating (up to 50°C after 10 s of exposure to near-infrared light). Lastly, multiple groups have developed self-lubricating organogels with τ_{ice} values as low as 0.4 kPa [102,103]. The gels consist of a low-modulus, lubricant-impregnated polymer network which contracts at low temperatures to expel a surface oil layer [102,103]. While they are vulnerable to mechanical damage, such surfaces illustrate the potential success of combined chemical and mechanical design strategies in lowering meso-scale ice adhesion.

As the length scale of the fouling ice increases, the success of surface design strategies becomes increasingly dependent on their consideration of the surface elastic modulus. For ice adhered to an elastic surface that it is able to deform, the de-bonding mechanism becomes distinct from that of ice on a rigid surface [104]. As was proposed by Kendall for pull-off of a rigid solid and later extended by Chaudhury to apply to shear detachment, the strength of a solid/elastic interface is governed by the relation $\sigma \propto \sqrt{W_a E/t}$ where W_a is the work of adhesion, E is the surface elastic modulus, and t is the surface layer thickness (figure 4*d*) [19–21]. Multiple groups have demonstrated that ice adhesion on such an elastic surface is a function of both surface energy (included in W_a) and surface modulus [105], as well as the thickness of a substrate [106,107]. However, in this region, it is the surface modulus which can be varied over the largest range. To allow macro-scale ice to be shed from a surface, extremely low values of ice adhesion are frequently necessary for a range of applications. For example, in order for a sheet of ice which measures 1 inch thick with 1 m^3 of contact area to passively detach from a typical offshore wind turbine, the ice adhesion strength of the surface must be $\tau_{ice} < 12$ kPa [108].

Beemer *et al.* [106] have demonstrated that cross-linked PDMS with an extremely low shear modulus of 10.3 kPa can yield an ice adhesion value of only $\tau_{ice} = 5$ kPa, which it retained after 100 icing/deicing cycles or 1000 abrasion cycles with 400 grit sandpaper. The impact of surface modulus on ice adhesion and durability has been studied most thoroughly by Golovin *et al.* [91]

who tested nearly 60 different compositions of elastomeric coatings to determine the impact of modulus, as well as imbedded miscible oil on surface ice adhesion and durability (figure 4*e*). They were able to generate multiple coatings with ice adhesion values as low as $\tau_{ice} = 0.15$ kPa, as well as exceptionally durable coatings with ice adhesion values of $\tau_{ice} < 10$ kPa that withstood damage from 100 repeat icing–deicing cycles, 5000 Taber abrasion cycles, thermal cycling and acid/base exposure [91]. They grouped elastic surfaces into three categories: no-slip surfaces, surfaces with interfacial slippage and lubricated surfaces. The no-slip condition, which applies to most surfaces, indicates that ice is rigidly adhered to the surface up until the moment of fracture. By filling low-modulus elastomers with a particular amount of oil, they can be rendered sufficiently mobile to allow ice to slip at its interface with the surface, without adding enough oil for the surface to become lubricated, i.e. form a free layer of oil on surfaces which leads to poor durability. In their follow-up work, the group proposed a design framework to predict the icephobic properties of polymeric surfaces, both thermoplastics and thermosets, based on the fraction of oil added, its miscibility and the inherent ice adhesion strength of the polymers [108]. Based on this framework, they fabricated icephobic coatings from a range of polymers such as polystyrene, polyvinyl chloride, natural rubber and polydimethyl siloxane.

In this section, we have summarized the different approaches in the literature that have been applied to the large commercial problem of ice fouling. This topic clearly demonstrates the need for a design framework dependent on the modulus and length scale of the fouling material, as the effective approaches for resisting ice fouling differ as a function of these parameters. The future of low ice adhesion surfaces rests on the development of higher durability surfaces prepared to meet the low-cost, high-scale demands of industrial use.

3. Clathrate fouling

Clathrates, or natural gas hydrates, occur when gas molecules become enclosed in the cage-like structures of water to form a crystalline material under conditions of high pressure and low temperature. The structure is stabilized by intermolecular forces, primarily hydrogen bonding and van der Waals interactions. Typical clathrate gasses include propane, methane, cyclopentane, ethane and carbon dioxide [36,109]. This class of materials poses a significant problem for oil and gas industries where hydrate accumulation inside pipelines can cause blockages, reduce flow and increase pressure build-ups, resulting in loss of production speed, increased energy costs and significant safety hazards [109,110]. Currently employed solutions to address this issue include the addition of methanol or glycol to a flow stream in order to shift its thermodynamic equilibrium, kinetic inhibitors to prevent hydrate nucleation or anti-agglomeration agents [110–113]. All of these additives present continual costs to operators, with annual worldwide methanol costs for this application reaching about $220 million in 2003 [113]. Additionally, flow compositions with high water content, or watercut, limit the effectiveness and exponentially increase the cost of these components [114].

The adhesion of clathrates to common pipe surfaces in a water-free environment is sufficiently low to allow de-bonding by natural flow forces alone [115]. However, Aspenes *et al.* have shown that in the presence of water, and especially in the case of a hydrated surface, the strength of clathrate–surface adhesion is as much as 10x stronger than clathrate–clathrate adhesion. Surfaces tested by the group included carbon steel, stainless steel, aluminium, brass, glass and epoxy [116]. As water is commonly present in oil and gas pipeline flows, this result demonstrates the clear need for investigations into low clathrate adhesion surfaces.

Within the context of the solid fouling surface design framework presented in figure 2, natural gas hydrates possess an elastic modulus on the order of 1 GPa [36,54] and exist on length scales ranging from nanoscale nucleation sites to macro-scale bulk fouling. Research on hydrate surface adhesion has focused on the meso-scale, using chemical functionalization to minimize surface energy. Smith *et al.* measured the adhesion of tetrahydrofuran hydrates to surfaces functionalized with a variety of silanes to achieve a range of surface energies. They found that a fourfold reduction in hydrate adhesion could be achieved by the lowest surface energy silane layer, which

minimized the work of adhesion [117]. Sojoudi *et al.* followed up on this work by measuring the adhesion of tetrahydrofuran hydrates and cyclopentane hydrates to CVD fabricated surfaces of polydivinylbenzene capped by poly(perfluorodecyl acrylate). Again, it was found that hydrate adhesion scaled with the work of adhesion of the surface, reaching as low as $\tau_{\text{clathrate}} = 20$ kPa [97,118].

Despite the high modulus of natural gas hydrates in the context of solid fouling materials, to the best of our knowledge, no work has been done to investigate the effects of surface modulus on meso- and macro-scale adhesion of these materials. Owing to the extreme similarity in modulus and chemical composition between ice and clathrates [36], it is reasonable to assume that many surface design strategies may be shared effectively between the two fouling scenarios. In fact, the CVD surfaces fabricated by Sojoudi *et al.* [97] were also applied to mitigate ice fouling; however, these surfaces were able to reduce ice adhesion strength to only $\tau_{\text{ice}} = 185.3$ kPa. In comparison, as discussed previously, durable, low-modulus surfaces achieved values of $\tau_{\text{ice}} < 10$ kPa [108]. Therefore, by considering the high modulus of this foulant and incorporating surface elasticity into low hydrate adhesion surface design, significant additional reduction in adhesion strength may be achieved.

4. Inorganic scaling

The deposition of inorganic scale [119] is a major challenge in a range of industries including oil and gas, water desalination and power generation [120–122]. The uncontrolled build-up of scale can cause flow restriction and increased friction in pipes (figure 5*a*), under-scale surface corrosion of metal parts and loss of heat transfer efficiency through fouled surfaces [120,122,126]. In water desalination applications, equipment design must allow as much as 40% additional heat transfer area to account for fouling by inorganic scale [127]. The costs incurred by industry as a result of scale fouling can be enormous, stemming from both operational losses and increased energy demands, as well as the continued maintenance of fouled systems [120,126]. Current approaches to combat inorganic scaling require mechanical removal and the use of chemical inhibitors to delay or prevent nucleation [120–122,126]. Mechanical approaches can be costly and are difficult to apply to many equipment configurations, especially without incurring significant equipment down time [120,121]. Chemical inhibitors and cleaning agents also present high costs, while introducing potentially damaging contamination to both products and the environment [120–122,126]. Consequently, the need for passive, antiscale adhesion surfaces is clear to limit costs and improve efficiency in a myriad of critical industries that use heat exchangers.

In order to place inorganic scale deposits within the fouling material framework presented in figure 2, it is critical to recognize that inorganic scaling exists over a broad size range, from microscopic nucleation sites to deposits which are inches thick with square metres of surface area. The modulus of inorganic scale is typically estimated from the modulus of $CaCO_3$, one of the most common scaling materials observed in industry [124]. With a value on the order of 10 GPa [55,56], $CaCO_3$ is the highest modulus fouling material addressed in this review. Therefore, the length scale of fouling will be critical in determining whether chemical- or modulus-based surface designs will have the greatest impact on reducing $CaCO_3$ adhesion strength.

Multiple surfaces have been proposed which use chemical functionalization to inhibit deposition during nucleation and early-stage adhesion. Research efforts have widely confirmed that reduction in the interfacial free energy of a surface results in: an increase in the final heat transfer coefficient for that surface in scaling environments [121,128], a reduction in the adhesion strength of scale deposits [120–122,124,126,129–131], a reduction in the nucleation rate of scale on the surface [120,124,130,132,133] and increased porosity of the scale deposits which do form (figure 5*b*) [126]. Specifically, multiple groups have identified the minimization of the polar component of the surface energy for a surface as the most impactful factor in limiting fouling [120,129]. Microscale roughness was found to increase both the rate of heterogeneous surface nucleation and the adhesion strength of deposited scale due to the increased surface area and mechanical locking effect of the impregnated texture [122,127,129,130,132–137]. Roughness also

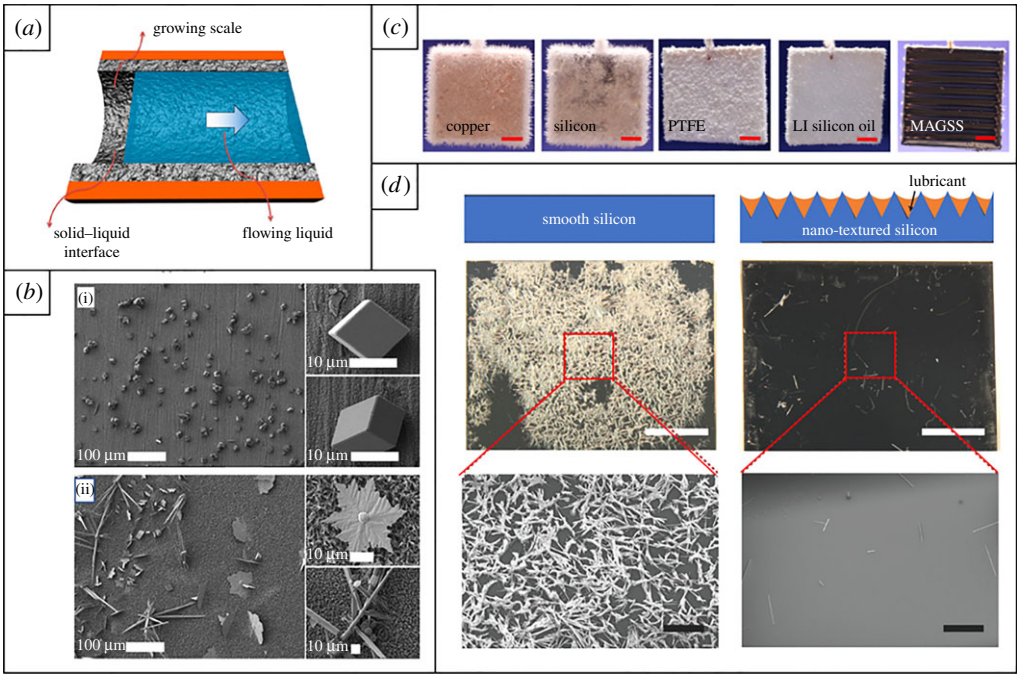

Figure 5. (*a*) A schematic illustrating scale deposition on the interior of a pipe. (*b*) SEM images of $CaCO_3$ crystals after 1 h of crystallization on samples of (i) pure Cu foil and (ii) superhydrophobic CuO nanowire film. (*c*) Forty-eight hours of calcium sulfate scale formation on copper, silicon, PTFE, liquid-infused silicon oil surfaces and MAGSS surface. The scale bar is 5 mm. (*a*, *c*) Adapted from [123] Copyright © 2017 American Chemical Society. (*b*) Adapted from [124] Copyright © 2015 American Chemical Society. (*d*) Calcium sulfate scale formation after approximately 80 h residence time on a smooth uncoated silicon substrate, and a lubricant-impregnated nanotextured silicon substrate. White scale bar 5 mm. Black scale bar 1 mm. (*d*) Adapted from [125] with permission.

led to higher density deposits due to enhanced nucleation density and the orientation of the crystals [135,136].

While some previous works reported low-energy surface designs that use SAMs [120,124] or fluorinated polymers [122,129,130,132], the harsh environmental conditions of heat transfer applications require that surface coatings be thermally conductive, heat-resistant, and resistant to mechanical abrasion [121,131]. Diamond-like carbon coatings have been used by multiple groups for this application because they are chemically inert, thermally conductive, durable and have low roughness values [128,130–132]. Zhao & Wang [131] demonstrated that fluorine-doped diamond-like carbon (DLC) can significantly reduce the adhesion of scale deposits. The electric double-layer theory states that the implantation of low metal character elements such as F, Si, H and C into a metal layer will reduce the ionic nature of its surface and consequently lower the surface energy [121]. Multiple groups have capitalized on this effect and demonstrated the correlation between low scale adhesion and increased elemental implantation into metal heat-exchanger parts [121,133,137]. Other ultra-durable, thermally conductive coatings in the literature include fluorine-doped tantalum carbide [128] and NI-P-PTFE composites [126,133].

Despite the high modulus of inorganic scale as a fouling material, and its frequent occurrence at relatively high length scales, to the best of our knowledge, no experimental literature exists on the effect of surface modulus on scale adhesion. This can be attributed to the unique requirements of conductivity, heat-resistance and mechanical durability for heat-exchanger coatings which eliminate virtually all elastic bulk materials from consideration. Müller-Steinhagen and Zhao reported that due to the thermal resistivity of polymeric materials, effective heat transfer

would require a coating thickness less than 5 µm [121], which would eliminate the impact of its elastic properties. As an alternative strategy, multiple groups have investigated lubricated surfaces, which possess a molecularly smooth surface to limit potential nucleation sites and a liquid surface interface to minimize scale adhesion. Subramanyam *et al.* [125] fabricated etched silicon samples impregnated with silicone oil and successfully demonstrated an over 48 h delay in scale nucleation, as well as a 10x reduction in adhesion strength when compared with bare silicon (figure 5*d*). Masoudi *et al*. demonstrated significant improvement in delaying scale nucleation, even over lubrication infused silicon oil substrates, by fabricating gel magnetic slippery surface (MAGSS). MAGSS are composed of styrene–ethylene–butylene–styrene triblock copolymer infused with a ferrofluid (figure 5*c*). These surfaces demonstrated scaling nucleation prevention for over 120 h under flow [123].

In this section, we have summarized multiple approaches in the literature which have been designed to address the issue of inorganic scaling. Ultimately, the future of low scale adhesion surfaces rests on the innovative development of high durability, high conductivity, heat resistant, low surface energy surfaces that can meet the low-cost, large-scale demands of industrial heat-exchanger applications.

5. Dust fouling

The adhesion of dust and particulate matter to surfaces represents another key type of solid fouling. Dust accumulation has the potential to dramatically reduce the output of solar panels by scattering and absorbing solar rays [138–143]. This impediment is particularly damaging in arid climates where infrequent rainfall and water shortages limit cleaning, high temperatures and dust storms exacerbate fouling, and low humidity increases static build-up [138,141,143,144]. Additionally, the heat transfer efficiency of heat exchangers in multiple industries is impacted by surface dust fouling, as well as the resultant air-side pressure drop within the exchanger [145,146]. Dust fouling has also been posed as a significant impediment to space science; expeditions to both the Moon and to Mars have experienced complications as a result of dust contamination [147–149]. While many self-cleaning surfaces have been developed which allow water to undercut adhered dust and rinse it from a surface [150–152], this review will focus only on the adhesion of dry dust as a solid foulant.

The elastic modulus of dust is virtually impossible to assign as the term encompasses particulates of a broad range of compositions. Dust primarily includes organic minerals, but also other materials such as pollen, hair or even human and animal cells [143]. What unites these components is their scale; dust particles are less than 500 µm in diameter [143]. This small length scale indicates that the chemical functionalization of a potential low adhesion surface is critical to its design. In 1980, Cuddihy [153] identified five surface properties which could be used to limit dust adhesion: hardness, roughness, hydrophobicity, surface energy and chemical cleanliness (particularly from water soluble salts). Of these, surface hydrophobicity/surface energy, as well as roughness, have been researched most thoroughly. Researchers have identified two primary factors influencing dust adhesion: van der Waals and electrostatic forces [147,153–156]. van der Waals interactions can be reduced by lowering a surface material's polarity and interfacial free energy, while electrostatic interactions are increased when surface charge induces coulombic interactions with particulates [147,153]. Additionally, Said *et al.* [141] demonstrated that the effect of surface texture depends strongly on its scale. Features larger than contaminating particulates will trap dust, while features on a smaller length scale limit the surface area which is presented for adhesion.

Jang *et al.* [139] used nanoscale texture, in addition to low-energy fluorinated surface functionalization to fabricate a superhydrophobic coating which reduced dust adhesion by 400% when compared with an untreated surface. Quan & Zhang [157] demonstrated that the texture required to achieve superhydrophobicity is not necessary to achieve dust repellency by fabricating and testing smooth tetraethoxysilane sol–gel coatings which minimize van der Waals effects and eliminate the risk of particle trapping. Multiple groups have confirmed that dust

adhesion scales with the interfacial free energy of the surface, primarily by testing low surface energy fluorinated surfaces [18,147,158].

Surface conductivity also plays a critical role in the reduction of dust fouling, as it prevents charge build-up which will increase electrostatic forces [143]. Dove *et al*. [147] demonstrated that conductivity can have a much larger impact on the attraction of dust particles than surface energy alone. Sueto *et al*. [156] created another conductive coating from a combination of WO_3 and partially hydrolysed tetraethyl orthosilicate and demonstrated low dust adhesion. Joseph *et al*. [155] demonstrated Indium Tin Oxide as a dust-repellant, conductive material with exceptional durability against abrasion, humidity, salt spray and thermal cycling. Fenero *et al*. [18] used laponite clay nanoparticles, partially functionalized with perfluoroalkylsilane, to fabricate an antidust surface which is both low energy and conductive. Continuing to investigate surfaces which are mechanically durable, low surface energy and conductive will enable researchers to improve the technology available to address the wide occurrences of dust fouling in both commercial and residential settings.

6. Paraffins and wax deposition

Wax and paraffin deposition can cause plugging of crude oil transportation pipelines and lead to production losses, cleaning downtimes and increased labour costs for oil and gas industries [159,160]. Much of the attention in petroleum fouling mitigation is given to deposit-inhibiting additives such as polymers [161], n-alkanes [162], wax crystal modifiers [163], dispersants [164,165] and even microbes [166,167]. However, such chemical additions to crude oil can be costly and require additional separation steps amidst an already complex and expensive purification process. Reports from field testing provide an indication of what pipeline coating strategies are commonly adopted, and offer clues for future antifouling strategies [168,169]. It is important to note that coatings designed to prevent wax deposition must withstand the harsh conditions inside of a petroleum pipeline, including severe abrasion, high temperature, high fluid shear stresses, and avoid chemical reactions with a myriad of organic compounds such as crude oil, resins, asphaltenes, waxes, scales, fines and water. Laboratory experimental designs in this case typically do not consistently mimic the technical complexities associated with on-site field application [170].

It is difficult to obtain a concrete modulus and length-scale range for paraffin waxes due to the diversity in their chemical composition, as a result of variability in processing conditions. However, reported values of modulus range between 61 and 250 MPa [51,52]. Although our design guide (figure 2) predicts that surface modulus and chemical functionality would have comparable effects on lowering the adhesion of foulants in this range of modulus, most efforts in the literature have been directed towards controlling surface free energy. The earliest antiwax coatings date back to the 1960s and use Bakelite lacquer, epoxy resins and enamel as a form of wax control [169,171]. Jorda investigated paraffin deposition on mill scale steel, as well as steel coated with smooth epoxy-phenolic and polyurethane coatings. They observed that after passing a wax-oil solution over these surfaces, less weight of paraffin was deposited on both of the smooth polymeric coatings, indicating an effect of both surface chemistry and texture on paraffin deposition [168].

Many early studies demonstrate surface energy and roughness as co-dependent factors in paraffin adhesion [168,172,173]. Quintella *et al.* [174] showed the dependence of wax deposition on the contact angle of a surface with paraffin oil. They observed high wax deposition rates for vinyl acetate copolymers with 28% oxygen content (EVA28) when compared with the more hydrophobic polymers, polypropylene (PP) and high-density polyethylene. Zhang *et al.* [175] tested paraffin deposition in crude oil for different surfaces. Low-energy surfaces such as polyvinylidene fluoride, poly(vinylidene fluoride)-chlorotrifluoroethylene and a methyl acrylate-styrene copolymer were tested and compared with higher surface energy polyurethane and epoxy surfaces. They demonstrated a decrease in paraffin deposition (of up to 75% compared to uncoated aluminium) with decreasing surface energy of the coating. They claimed that a

combination of surface composition, chemical functionality and surface density of the functional groups affects wax wettability as measured by contact angle hysteresis with crude oil. This in turn controls the work of adhesion of paraffin on the surface. Rashidi *et al.* [176] recently showed approximately 86% reduction in grams of paraffin wax deposition from Malaysian (Tapis) crude oil on ethylene-tetrafluoroethylene versus steel and PVC. Finally, substrates coated with DLC (surface energy of approx. 30 mN m^{-1}) also allow for low paraffin deposition, with the additional advantages of being able to withstand the harsh abrasive and thermal environments within an oil pipeline [177].

The impact of surface energy has been typically investigated within the context of mass deposition rates of wax and paraffin on different industrial surfaces, as opposed to direct surface-wax bond/adhesion measurements. Our design framework suggests that alteration of surface modulus may offer an avenue for continued improvement. Further research into the correlation between coating stiffness and wax deposition rates, as well as bond adhesion, may demonstrate the benefits of lowering modulus and perhaps offer avenues to use the synergistic advantages of low surface energy, highly elastic materials. The high durability demands for surfaces applied to oil transportation pipelines will likely present the greatest hindrance in this development.

7. Protein fouling

The contamination of surfaces by biological matter and organisms, or biofouling, is problematic for a multitude of fields and applications [119]. Within the medical realm, biocontamination can be dangerous for implants [178–181], surgical equipment [182–184], catheters [185–188] and hospital beds [189]. Biofouling is also problematic for food packaging and storage [190–193], filtration [194–198], as well as marine vessels [1,199,200] and infrastructure [201,202]. It is therefore imperative to develop antifouling surfaces which resist the attachment of biological organisms.

Unlike other forms of undesired solid adhesion, biological fouling is multiphasic, with each phase building on, or aiding the next. Biological organisms also possess the ability to divide, and to adjust based on the properties of the underlying surface [203]. The fouling process typically begins with protein adsorption on a surface, which serves as a conditioning layer for larger order organisms [203–205]. This process can occur within seconds, or minutes [203]. Besides acting as a conditioning layer for attachment of larger organisms, the adsorbed proteins can hamper the performance of immunological assays [206,207], lead to thrombosis for medical implants [208,209] and aid in the formation of platelets within certain microfluidic devices [208]. It has been demonstrated that even 10 ng cm^{-2} of the protein fibrinogen adsorbed on a surface can lead to blood platelet formation [208]. Surface design should thus be focused not only on the reduction in large bio-organisms, but also on protein fouling independently.

Proteins are complex biomaterials which consist of one or more ordered polypeptide chains [210]. These polypeptides can have a wide array of functionalities, causing either hydrophilic or hydrophobic character. Within aqueous solutions, proteins take on a metastable globular form where the majority of the hydrophobic functionality is ordered within the interior, while the hydrophilic side groups are oriented to the exterior [210]. The metastability of proteins is a result of a decrease in conformational entropy for the ordered interior non-polar groups which is somewhat overcome by their hydrophobic interactions, as well as by the enthalpic stabilization of the outer hydrophilic groups by surrounding water molecules [210]. This makes proteins susceptible to chemical, thermal or mechanical perturbations, which can lead to unfolding, and adsorption. Low surface energy hydrophobic surfaces, although able to repel high surface tension fluids, will cause protein adsorption by disrupting their metastable state. Additionally, even though proteins vary broadly in modulus [211,212], their small length scales do not allow for the low surface modulus approaches previously discussed to be a sufficient solution to combat adhesion. Regardless of the inherent challenges, chemistry-based approaches can be useful in rendering certain surfaces protein-resistant.

Poly(ethylene glycol) (PEG)-based grafted polymers are among the most commonly studied surface treatments used for the prevention of protein adsorption [213–221]. Jeon *et al*. [213] were

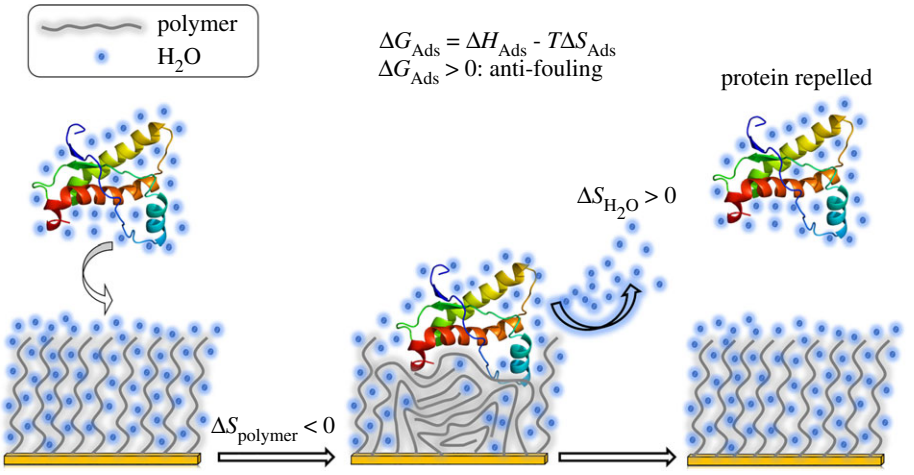

Figure 6. Protein repellency mechanism for a hydrophilic, brush-like grafted polymer [210,213,219]. Protein adsorption onto grafted PEG results in the release of the hydration barrier from both the polymer and the protein. This process increases the entropy for water, but is outweighed by a decrease in conformational entropy for the polymer. The net result is entropically unfavourable for protein adsorption. (ΔH_{Ads}) for the protein–polymer interaction can either be favourable or unfavourable depending on the paired species [210,222]. More strongly bound water results in less favourable protein adsorption.

one of the first groups to study the antifouling characteristics of grafted PEG. With a simple model, the group found that as a protein approaches a substrate, the PEG chains are compressed, leading to a decrease in conformational entropy, translating to compressive elastic forces [213]. Water molecules attracted to the hydrophilic PEG are displaced as a result of this compression, leading to a thermodynamically unfavourable osmotic barrier [207]. The coupling of both forces acts as a net repulsive force to the incoming proteins [213,219]. Figure 6 illustrates this process. The extent to which proteins will not adsorb to the surface monotonically increases with an increase in PEG grafting density and chain length [213]. Jeon *et al.*'s theoretical findings were later confirmed with a more refined model [219], validating the importance of grafting density, chain length, and polymer chain hydrophilicity.

Using SAMs, Prime and Whitesides were able to attach high grafting density monolayers presenting oligo(ethylene oxide) terminal groups onto gold substrates [207,214,223]. An array of proteins was introduced to the fabricated surfaces to prove the surface's protein resistance. These proteins included: fibrinogen, pyruvate kinase, lysozyme, and ribonuclease [223]. All tested proteins were repelled by the SAMs [223]. Contrary to previous studies claiming the importance of long grafted chain lengths, high-density SAMs presenting only two monomer groups of ethylene oxide displayed notable protein resistance [223]. This discovery does not contradict the theory proposed by Jeon *et al*. [213,219], as it demonstrates the importance of high grafting density which was previously fulfilled by substantially longer PEG chains [207]. Additionally, this finding reinforced the importance of polymer hydrophilicity in order to create a hydrated barrier for impinging proteins.

To take this understanding further, many groups have studied zwitterionic grafted polymers to impart protein resistance [13,15,16,224–226]. Zwitterionic polymers tightly bind to water due to the strong dipole created by anionic moieties [228]. It has also been suggested that the structure of zwitterionic groups forces water into a highly ordered array [229]. As a consequence, relatively high amounts of energy are required to disrupt the organized water molecule network supported by the zwitterionic moieties (figure 7*a*) [229]. Early studies were conducted by Holmlin *et al.* [15] and Tegoulia *et al.* [224] on the protein fouling resistance of phosphorylcholine-based zwitterionic SAMs. As expected, both groups observed low comparative levels of protein adsorption on the zwitterionic SAMs due to the strongly bound hydration layer. Chang and co-workers [225]

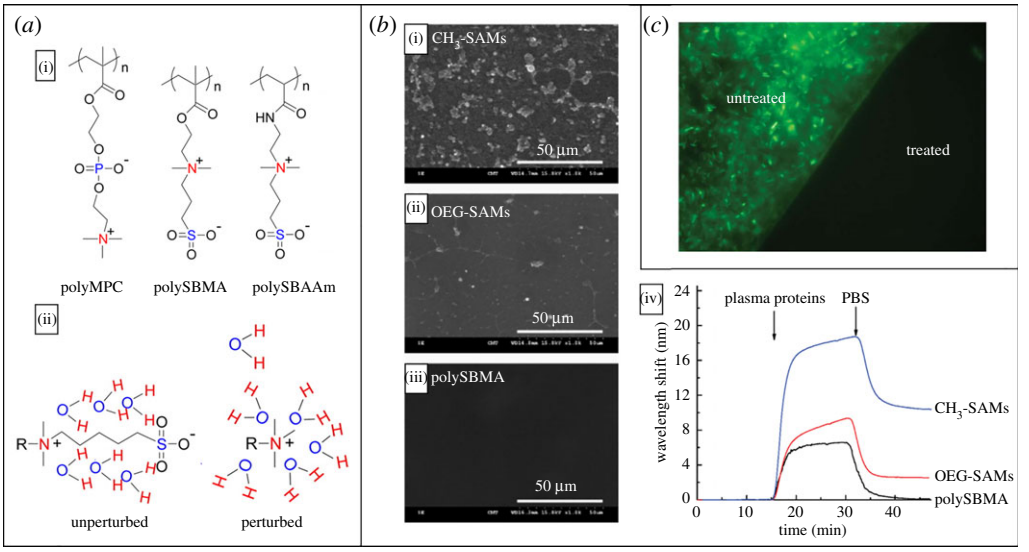

Figure 7. (*a*)(i) Three examples of zwitterionic polymers: poly-(methacryloyloxylethyl phosphorylcholine), polyMPC; poly-(sulfobetaine methacrylate), polySBMA; and poly-(sulfobetaineacrylamide), polySBAAm. (ii) Graphic representation of two ordering mechanisms for water by a charged group, and zwitterionic group. The zwitterionic polymer allows water's highly ordered structure to remain 'unperturbed', while a single charge disrupts the hydrogen bonds of water into a more disordered state. Images adapted from [229] and reprinted with permission Copyright © 2014 American Chemical Society. (*b*)(i–iii) Minimization of platelet adhesion by using zwitterionic polySBMA SAMs when compared with SAMs presenting terminal methyl and oligo(ethylene glycol) groups. (iv) An SPR plot comparing adsorption of blood plasma proteins at 37°C. A 1 nm wavelength shift is equivalent to a deposition of 15 ng cm^{-2}. Images adapted from [227] with permission. Copyright © 2008 American Chemical Society. (*c*) Fluorescence microscopy image displaying *Pseudomonas aeruginosa* attached to a partially coated NH_2-glass substrate after 70 h of bacterial exposure. A section of the surface was treated with a zwitterionic polymer pSBMA300-catechol (treated) while a portion of the surface remained unmodified (untreated). Adapted from [16] with permission. Copyright © 2009 John Wiley and Sons.

studied blood plasma and platelet adsorption to zwitterionic grafted surfaces, as well as methyl and oligo(ethylene glycol) terminated SAMs [226]. The group observed ultra-low levels of both platelet and blood plasma proteins adsorbed to the zwitterionic surface when compared with the controls. Scanning electron microscopy and surface plasmon resonance (SPR) were used to confirm these findings (figure 7*b*). Beyond protein antifouling, grafted zwitterionic polymers have displayed notable long-term bacterial resistance as shown by multiple groups [14,230–232]. Li *et al.* [232] developed a sophisticated, easily applied, bacteria- and protein-resistant zwitterionic polymer termed pSBMA300-catechol. This polymer, when grafted to NH_2 functionalized glass, resisted the adsorption of a wide range of proteins, in addition to bacteria over a 70 h period (figure 7*c*) [232]. Zwitterionic polymers have also proven to be more robust than PEG and are not limited to being implemented as a weakly bound SAM [233–238]. Moreover, PEG auto oxidizes within air and aqueous solutions into aldehyde-terminated chains, severely diminishing its protein resistance [238]. Zwitterionic grafted polymers thus have proven to be an overall advantageous route to achieving durable, long-term, protein- and bacteria-resistant surfaces.

8. Polymer fouling

Unlike protein fouling, organic polymer fouling has been infrequently studied. Polymer fouling can lead to: contamination during polymerization reaction processes [239], down time during reactor cleaning cycles [239], ineffective filtration [240] and inefficient heat exchangers [241].

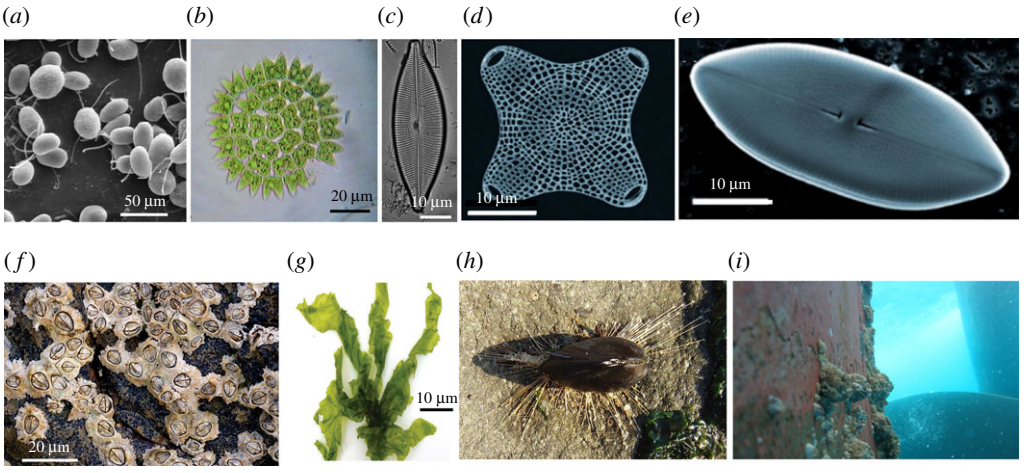

Figure 8. Images highlighting the diversity of marine foulants, including (*a*) SEM image of green algae, adapted from (http://remf.dartmouth.edu/imagesindex.html under public domain notice), (*b*) non-motile coenobium (group of cells) of *Pediastrum duplex*, a species of freshwater green algae, licensed under (https://creativecommons.org/licenses/by-sa/3.0/deed.en). (*c*) Diatom frustule of *Cymbella inaequalis* (adapted with permission from [244]). (*d*,*e*) SEM images of marine diatom species (adapted with permission from [245]). (*f*) *Chthamalus stellatus* barnacle photographed near the upper shoreline, Lundy Island, UK, reproduced with permission from (https://creativecommons.org/licenses/by-sa/3.0/deed.en). (*g*) *Ulva lactuca* a.k.a. sea lettuce (adapted from [246]. Copyright © 2014 licensed under https://creativecommons.org/licenses/by/3.0/). (*h*) A mussel (genus *Mytilus*), attached to a rock by its secreted filaments called byssus, licensed under https://creativecommons.org/licenses/by-sa/3.0/deed.en. (*i*) Biofouling on a ship hull adapted from [35] licensed under https://creativecommons.org/licenses/by/4.0.

In biological settings, algae and diatoms secrete extracellular polymeric substance (EPS) when adhering to a given surface [205,242]. EPS strengthens their attachment, but can be problematic for a variety of marine applications [205,242]. Polymers in solution, although unlike the metastable proteins, exhibit a similar surface repellency mechanism shown in figure 6. Organic fouling within an organic solvent was studied extensively by Wang *et al*. [243]. The group investigated the comparative polymer repellency of a single fluorine atom terminated alkyne monolayer, with alkyne monolayers containing 17, 3 and 0 fluorine atoms [243]. The single fluorine terminated monolayer proved to be highly repellent to a broad range of polymers with varying functionalities [243]. This finding closely matches the models proposed for protein adsorption as the strong dipole created by the single fluorine terminated monolayer strongly attracted the dimethylformamide (DMF) solvent, creating a barrier to adsorption of polymer chains. The single fluorine atom monolayer did however foul when encountering P2VP/DMF [243]. As confirmed by simulations, the interaction between protonated pyridine moieties, and polarized C–F groups was strong enough to break through the solvent layer and overcome the decrease in conformational entropy of the grafted monolayer [243]. The study of polymer antifouling in solution is still in its infancy, allowing for new opportunities to develop techniques to mitigate this phenomenon.

9. Marine fouling

Marine fouling materials are a special class of foulants in that they represent a diverse community of organisms with varying sizes, preferences to surface settlement, attachment as well as release mechanisms (figure 8*a*–*i*). This causes marine fouling to be time-dependent, and possess a unique evolutionary attachment sequence. Marine organisms are an important part of the biosphere;

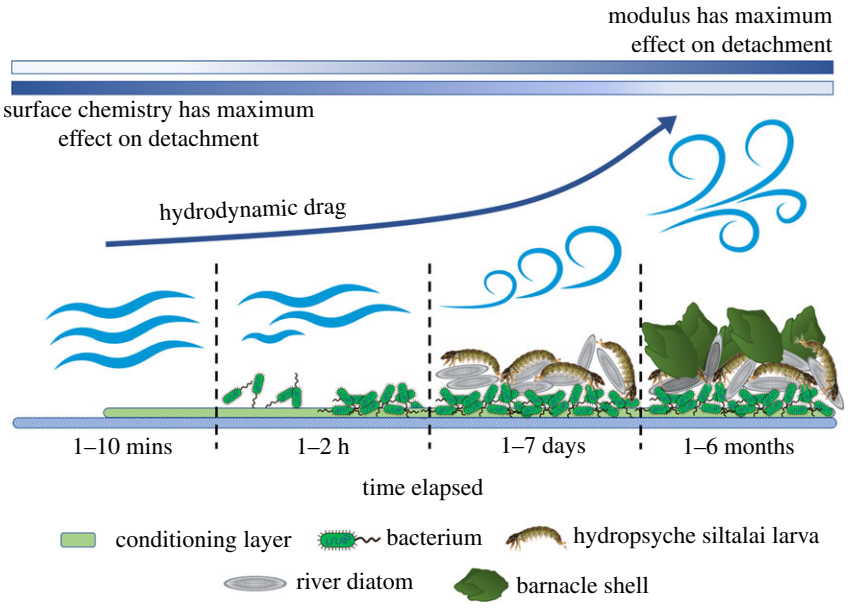

Figure 9. The marine fouling sequence observed on a surface underwater. Within the first few minutes, a layer of organic macro-molecules, known as the conditioning layer, is formed and fouls the surface [242,249,250]. After 1-2 h of submersion, planktonic bacteria colonizes the conditioning layer [250]. Within several days, the substrata become a habitat for larger unicellular organisms such as diatoms [205,242] followed by multicellular species of larvae, algae and algae spores (image licensed under https://creativecommons.org/licenses/by/3.0/deed.en). After several weeks, the surface experiences fouling from increasingly complex organisms such as tunicates, mussels and barnacles [205,251]. A consequence of fouling on a ship hull is the increased drag experienced by the vessel in motion which increases costs and extends downtime during hull maintenance [200].

however, they can be highly damaging to underwater sensors and increase drag experienced by marine vessels several fold [247,248]. This in turn raises their fuel consumption [1,200], and environmental pollution. Furthermore, ship maintenance for removal of these organisms extends down time and cleaning expenditures [1]. When a surface is submerged underwater in a marine environment, it provides a fresh surface on which an ecosystem can develop. First, an organic layer composed of humic acids, uronic acids, carbohydrates, amino acids and proteins is formed within the first few minutes of fouling [242,249,250]. This film provides an 'environment signal' that activates production of the necessary genes, proteins or even structural changes [250] (metamorphosis) that encourages planktonic bacteria attachment on top of the film. This attachment in turn provides a nutrition layer for unicellular organisms such as protozoa and diatoms which bind via mucus or EPS secretion [205,242]. This surface environment becomes a breeding ground for multicellular species of larvae, algae and algae spores which colonize within several days, followed by increasingly complex organisms such as tunicates, mussels and barnacles over the course of several weeks [205,251]. It is this dependence on foulant size, geographical location and time that makes marine fouling (figure 9) an intractable issue to solve.

(a) Microbial fouling

One solution to marine fouling that has been explored previously is blocking the initial food supply for the fouling species, namely proteins and bacteria [207,252]. Given the extremely low modulus of biofilms, between 10 Pa and 600 kPa [30–32,253,254], these foulants are incapable of deforming any reasonably robust solid substrate. Therefore, consistent with our guiding framework, the role of surface functionalization has been extensively studied to mitigate initial

bacterial or protein attachment onto a surface [252,255,256]. The relationship between bacterial retention on a surface and the surface energy of the substrata is well represented by the Baier curve [257]. For many attached biofouling organisms present in numerous natural environments (bacterial suspensions, fresh, brackish and sea water), minimum fouling is achieved between a substratum surface energy of $\gamma_{sv} \sim 20$–$30\,\mathrm{mN\,m^{-1}}$. This surface energy is approximately equal to the dispersive force contribution of water (approx. $22\,\mathrm{mN\,m^{-1}}$ and $50\,\mathrm{mN\,m^{-1}}$ for the dispersive and polar force contributions, respectively). Hence, the thermodynamic cost for water to wet a solid (from a hydration layer) with surface energy of approximately $22\,\mathrm{mN\,m^{-1}}$ is minimum [257]. If much higher or lower surface energy materials are selected, fouling would be more likely.

Several groups continue to investigate the utility of low surface energy of materials such as polydimethylsiloxane (PDMS) and fluorinated polymers, as foul-release (FR) coatings [258,259]. Hydrophobic antifouling coatings, such as Intersleek 1100SR, work by exploiting a fluorinated, low surface energy material that minimizes the surface interaction with slime and subsequent foulants. However, such a design is only effective in dynamic operation (i.e. when a marine vessel is moving) and not for extended static conditions, when the ship may be docked. During docking, such surfaces can be fouled by the adhesion of complex and hard organisms, significantly increasing the ship drag [247,258]. The argument for hydrophilic surfaces is that the presence of a strongly bound hydration layer will prevent the attachment of foulants. A good example is the Hempasil X3 FR paint which forms a water-retaining PDMS hydrogel network and shows less attachment to marine foulants compared to PDMS and a PDMS coating with fluorinated oils [260]. As discussed previously, zwitterionic polymers work by a similar principle in that they develop a hydration layer that inhibits bacterial attachment by diminishing electrostatic interactions [261–263]. Additionally, the effect of surface chemistry seems to be species-dependent, i.e. one type of foulant may adhere better than another for a particular surface [264–266]. Nonetheless, appreciable removal of organic molecules and microorganisms depends more strongly on fine tuning of surface chemistry than on the surface physical properties such as stiffness. Bakker *et al.* [267,268] showed minor but observable decreases in the attachment of marine bacteria while lowering the modulus of stiff substrates (from 2.2 to 1.5 GPa). Unless the surface modulus is lowered sufficiently to render marine foulants capable of deforming the fouling surface ($E < 50\,\mathrm{kPa}$), the stiffness of the substrate will not affect adhesion to an observable extent [269,270].

(b) Diatomaceous fouling

There is considerable literature agreement with the strategy to arrest the initial settlement of larger single-celled microorganisms such as diatoms and protozoa [250,258,271]. Species of diatoms such as *Navicula pelliculosa* were found by nanoindentation to have a hard shell (called a frustule) with modulus varying from 7 to hundreds of GPa, similar to silicas [272,273]. Losic *et al.* [274] reported an elastic modulus of approximately 3.4 GPa for *Coscinodiscus* sp. diatom frustule's perforations. The diatom frustule, or outer shell, is hard with softer mucilage layers underneath (figure 10). Diatoms can bind on different surfaces by secreting mucilage consisting of EPS [275]. Higgins *et al.* [276] have reported the elastic modulus of the softer mucilage (secreted fluids enabling attachment) layers in *Pinnularia viridis* and *Craspedostauros australis* diatoms to be between 0.54–0.76 and 0.25–0.45 MPa, respectively. Marine and freshwater diatoms span minute sizes from 10^2 to $10^9\,\mu\mathrm{m}^3$ and 10 to $10^6\,\mu\mathrm{m}^3$, respectively [277]. At this length scale, based on figure 2, limiting the adhesion of these foulants will again require the tuning of surface chemistry.

Amphiphilic coatings, which possess both hydrophobic and hydrophilic domains, disturb the settlement of hydrophobic and hydrophilic foulants such as *Navicula* diatoms and *Ulva linza* zoospores, respectively. Krishnan *et al.* [266] used block copolymers with ethoxylated fluoroalkyl side chains and outperformed PDMS surfaces in lowering adhesion for these two species. Several other reports also demonstrate the utility of using amphiphilic polymer coatings to reduce the attachment of different marine species [278–282].

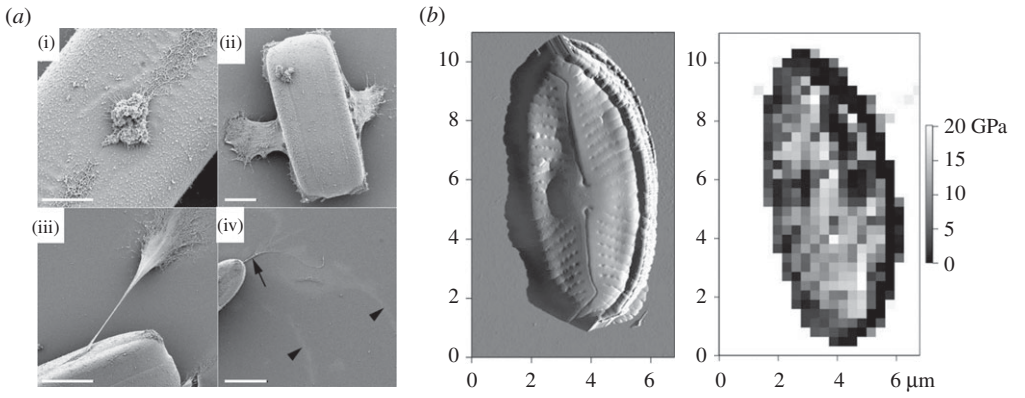

Figure 10. (*a*) SEM of chemically fixed *Pinnularia viridis* cells after settling for 30 min on the substratum (glass coverslips). (i) A large mass of mucilage (sticky substance) that is tenuously attached along the diatom slits (called raphe) is observed at the centre (central nodule). (ii) Two sheets of mucilage that extend down from the diatom to form a connection with the substratum. (iii) A long thin mucilaginous tether extending from the diatom surface and forming a connection with the substratum. (iv) The tethers are observed on the substratum (arrow), in addition to fine diffuse trails that form curved patterns (arrowheads). Scale bars: 5 mm (*a*(i)), 10 mm (*a*(ii)), 15 mm (*a*(iii) and *a*(iv)) (adapted with permission from [273]). (*b*) Atomic force microscopy mapping of a diatom shell (frustule) showing modulus values at different locations. A region of stronger material spans along the centre of the body (reproduced with permission from [45]).

Since most marine foulants are organic, free radical or reactive oxygen species generators may be useful in causing their degradation and thereby reduce fouling. Free radical generators such as titanium dioxide, zinc oxide and tungsten oxide have been previously used to reduce fouling. Although they are usually equipped with photosensitizer dyes to induce more efficient absorption of light, their performance is limited by that incident light's intensity [207]. Another mechanism to cause degradation is biocide deployment. Zargiel *et al.* published an extensive study on the multi-species diatom fouling of a myriad of coatings including commercial foul-releasers, copper-based surfaces and non-copper biocidal coatings. They found that certain diatoms like *Amphora* adhere more strongly to FR coatings than on biocide-based coatings demonstrating the inefficacies of modern FR coatings [271]. Commercial coatings, such as Hempaguard X7, use copper pyrithione as a biocide and provide ship protection from fouling marine organisms for up to 120 idle days of operation [283]. Dow's Sea-Nine™ coating is functionalized with biocidal 4,5-dichloro-2-*n*-octyl-4-isothiazolin-3-one, and targets the adhesion of diatoms, freshwater and marine bacteria, algae, and barnacles. This material displays rapid biodegradability when compared with previously used toxic biocides such as tributyltin (TBT) [284]. However, the biocide is still toxic to numerous non-target species such as tunicates [285]. Several attempts have been made in developing other less toxic biocidal antifouling paints, however, such biocides display varied toxicity among the mixed diatom community [271]. Researchers have also investigated the integration of biocidal and foulant-release coatings. However, getting the biocide to be miscible within the FR silicone polymer networks has proven to be extremely challenging and has hindered this approach [258].

(c) Macro-fouling

For the prevention of macro-scale biofouling, surface chemistry has been observed to have a limited effect on fouling, while the modulus of the substrate begins to have a more important role (as shown in figure 2). Barnacle and mussel adhesion is a complex process, involving the attachment of proteins to any organic substrata via high strength covalent bonding [286]. Lowering the modulus of an elastic foulant-release coating has been shown by several researchers

as an effective deterrent against algal plants [33] and barnacles (or pseudo-barnacles) [20,34]. A significant decrease in detachment force was observed when the coating modulus was reduced 10–1000 times lower than the foulant modulus [20,33,34,287–289]. Chaudhury *et al.* observed that the attachment of *Ulva* sporelings (young plants) was reduced by approximately 80% when modulus of a PDMS coating was reduced 12-fold. The attachment of *Ulva* spores (size approx. 5–7 µm), however, required a 47-fold reduction in modulus to observe the same per cent detachment [33]. The reason for this is that the sporelings have a well-developed cell wall that increases their overall rigidity. Shultz *et al.* showed increased removal of *Enteromorpha* biofilms under shear as they grew in size over a 6-day growth period over a surface coated with Veridian (a commercial FR coating from International Paint). They observed approximately 90% removal for 6-day-old biofilm compared to only approximately 15% removal for 1-day-old biofilm [290]. This shows that FR becomes more prominent for larger biofilms due to increased hydrodynamic shear, as the film grows larger.

The problem of marine fouling draws participation from species of varying sizes and modulus. Minute foulants including soft organic layers and bacteria are incapable of appreciably deforming the coating surface. Therefore, the modulus of the underlying substrata has a much lower effect on settlement and adhesion of such foulants when compared with tuning substrata surface chemistry, which has proven to be the most effective pathway in fouling mitigation. Owing to the vastness in fouling species present in the aquatic environment, with preferential adhesion and breadth in size and rigidity, a single antifouling solution currently does not exist. As for much larger macro-foulants, such as algal plants, barnacles and mussels, and smaller but harder micro-foulants, such as diatoms, substrata stiffness starts to contribute to adhesion as well. An antifouling coating would thus need to have a modulus that is significantly lower than these foulants. However, the coating stiffness must be sufficiently high to maintain durability requirements during its operation lifetime. Hence, extremely soft materials would not suffice as a feasible coating option.

10. Conclusion

In this review, we have broadly discussed solid fouling, and the various surface design solutions required for effective prevention. Fouling, defined as the undesired adhesion or adsorption of solid contaminants to a given surface, included but was not limited to: ice, scale deposits, wax and asphaltenes, polymers, dust and a complex range of biological matter and organisms. Each form of solid fouling is problematic or dangerous for multiple applications and industrial processes. Some examples covered in this text include ice on airplane wings, clathrates in industrial oil and gas piping, barnacles and mussels on ship hulls, scale on heat exchangers, dust formation on solar cells and protein adsorption to medical implants.

No single engineered surface has been developed which can broadly solve the problem of solid fouling. Many groups have designed surfaces to combat fouling, but typically only a single fouling material is studied at a time. However, certain similarities between each study can help draw a relation between the foulant size and modulus, and the most effective direction for antifouling surface engineering. At small length scales, ice and calcite nucleates, bacteria, algal spores and proteins may be repelled or greatly inhibited by surfaces with carefully designed chemistries. Lowering the surface free energy is often sufficient to reduce fouling at this scale; however, biological matter such as proteins are most effectively repelled by high surface energy molecular brushes. Regardless, the antifouling effects of chemistry-based design approaches dominate for relatively small-scale foulants. Larger fouling scenarios such as ice sheets, barnacles and calcite deposits benefit from low-modulus surfaces for facile de-bonding. These foulants when large enough can elastically deform a rigid surface when under an applied force, and therefore benefit from low-modulus surfaces which reduce the surface elastic energy during the de-bonding process. Some materials with intermediate size or modulus, including diatoms, barnacles and small ice nucleates, may require surface designs which consider both chemistry and elastic modulus for non-fouling surface properties. For example, some diatom species have

lengths on the order of micrometres, but possess a high modulus shell that could reach hundreds of GPa. Diatoms and other foulants of this nature therefore require surfaces with low modulus and fine-tuned chemistry for antifouling properties. Thus, there remains an interplay between the foulant modulus and size which dictates the final surface engineering considerations.

To conclude, we have broadly reviewed many modes of solid fouling, as well as the surface design strategies in the literature which have demonstrated effective prevention and/or release. Design considerations primarily include the intrinsic modulus and the length scale of the foulant, as well as the chemical functionality and elastic modulus of the surface. For many situations, when a foulant is low in modulus and relatively small in dimension, chemistry-based approaches to prevent fouling are dominant. Conversely for larger, more rigid forms of fouling, a low-modulus surface will tend to be most effective for facile removal. Many real-word applications constrain this framework further with the need for a surface to resist high temperatures, chemical damage and mechanical deformation. Therefore, surface durability offers a critical dimension to be implemented within our framework. Many groups have made great strides in the development of durable antifouling surfaces for a range of different applications, and with this continuous progress, we look forward to new developments which will significantly impact this important area.

Data accessibility. This article has no additional data.

Authors' contributions. All authors drafted, read, edited and approved the manuscript.

Competing interests. We declare we have no competing interests.

Funding. We thank Dr Ki-Han Kim and the Office of Naval Research (ONR) for financial support under grant no. N00014-12-1-0874. We also thank Dr Kenneth Caster and the Air Force Office of Scientific Research (AFOSR) for financial support under grant no. FA9550-10-1-0523. We also thank the National Science Foundation and the Nanomanufacturing program for supporting this work through grant no. 1351412.

References

1. Schultz M, Bendick J, Holm E, Hertel W. 2011 Economic impact of biofouling on a naval surface ship. *Biofouling* **27**, 87–98. (doi:10.1080/08927014.2010.542809)
2. Schultz M, Walker J, Steppe C, Flack K. 2015 Impact of diatomaceous biofilms on the frictional drag of fouling-release coatings. *Biofouling* **31**, 759–773. (doi:10.1080/08927014.2015.1108407)
3. Agency EP. 2012 Effluent limitation guidelines and new source performance standards for the airport deicing category, p. 37. Federal Register.
4. Gent R, Dart N, Cansdale J. 2000 Aircraft icing. *Phil. Trans. R. Soc. Lond. A* **358**, 2873–2911. (doi:10.1098/rsta.2000.0689)
5. Laforte J, Allaire M, Laflamme J. 1998 State-of-the-art on power line de-icing. *Atmos. Res.* **46**, 143–158. (doi:10.1016/S0169-8095(97)00057-4)
6. Aiyejina A, Chakrabarti DP, Pilgrim A, Sastry M. 2011 Wax formation in oil pipelines: a critical review. *Int. J. Multiphase Flow* **37**, 671–694. (doi:10.1016/j.ijmultiphaseflow.2011.02.007)
7. Leontaritis KJ, Mansoori GA. 1988 Asphaltene deposition: a survey of field experiences and research approaches. *J. Petrol. Sci. Eng.* **1**, 229–239. (doi:10.1016/0920-4105(88)90013-7)
8. Donlan RM. 2001 Biofilms and device-associated infections. *Emerg. Infect. Dis.* **7**, 277. (doi:10.3201/eid0702.010226)
9. Percival SL, Suleman L, Vuotto C, Donelli G. 2015 Healthcare-associated infections, medical devices and biofilms: risk, tolerance and control. *J. Med. Microbiol.* **64**, 323–334. (doi:10.1099/jmm.0.000032)
10. Chaudhury MK. 1996 Interfacial interaction between low-energy surfaces. *Mater. Sci. Eng.: R: Rep.* **16**, 97–159. (doi:10.1016/0927-796X(95)00185-9)
11. Packham DE. 2003 Surface energy, surface topography and adhesion. *Int. J. Adhes. Adhes.* **23**, 437–448. (doi:10.1016/S0143-7496(03)00068-X)
12. Callow ME, Fletcher RL. 1994 The influence of low surface energy materials on bioadhesion—a review. *Int. J. Biodeterior. Biodegred.* **34**, 333–348. (doi:10.1016/0964-8305(94)90092-2)

13. Chen S, Zheng J, Li L, Jiang S. 2005 Strong resistance of phosphorylcholine self-assembled monolayers to protein adsorption: insights into nonfouling properties of zwitterionic materials. *J. Am. Chem. Soc.* **127**, 14 473–14 478. (doi:10.1021/ja054169u)
14. Cheng G, Zhang Z, Chen S, Bryers JD, Jiang SJB. 2007 Inhibition of bacterial adhesion and biofilm formation on zwitterionic surfaces. **28**, 4192–4199. (doi:10.1016/j.biomaterials.2007.05.041)
15. Holmlin RE, Chen X, Chapman RG, Takayama S, Whitesides GM. 2001 Zwitterionic SAMs that resist nonspecific adsorption of protein from aqueous buffer. *Langmuir* **17**, 2841–2850. (doi:10.1021/la0015258)
16. Jiang S, Cao Z. 2010 Ultralow-fouling, functionalizable, and hydrolyzable zwitterionic materials and their derivatives for biological applications. *Adv. Mater.* **22**, 920–932. (doi:10.1002/adma.200901407)
17. Baytekin HT, Baytekin B, Hermans TM, Kowalczyk B, Grzybowski BA. 2013 Control of surface charges by radicals as a principle of antistatic polymers protecting electronic circuitry. *Science* **341**, 1368–1371. (doi:10.1126/science.1241326)
18. Fenero M, Palenzuela J, Azpitarte I, Knez M, Rodríguez J, Tena-Zaera R. 2017 Laponite-based surfaces with holistic self-cleaning functionality by combining antistatics and omniphobicity. *ACS Appl. Mater. Interfaces* **9**, 39 078–39 085. (doi:10.1021/acsami.7b13535)
19. Chaudhury M, Kim K. 2007 Shear-induced adhesive failure of a rigid slab in contact with a thin confined film. *Eur. Phys. J. E* **23**, 175–183. (doi:10.1140/epje/i2007-10171-x)
20. Chung JY, Chaudhury MK. 2005 Soft and hard adhesion. *J. Adhesion* **81**, 1119–1145. (doi:10.1080/00218460500310887)
21. Kendall K. 1971 The adhesion and surface energy of elastic solids. *J. Phys. D: Appl. Phys.* **4**, 1186. (doi:10.1088/0022-3727/4/8/320)
22. Popov VL. 2010 *Contact mechanics and friction*. Berlin, Germany: Springer.
23. Chen Z, Nosonovsky M. 2017 Revisiting lowest possible surface energy of a solid. *Surf. Topogr.* **5**, 045001. (doi:10.1088/2051-672X/aa84c9)
24. Callister D, Rethwisch DG. 2007 *Materials science and engineering: an introduction*, 7th edn. New York, NY: John Wiley and Sons, Inc.
25. Johnston I, McCluskey D, Tan C, Tracey M. 2014 Mechanical characterization of bulk Sylgard 184 for microfluidics and microengineering. *J. Micromech. Microeng.* **24**, 035017. (doi:10.1088/0960-1317/24/3/035017)
26. Tuteja A, Choi W, Mabry JM, McKinley GH, Cohen RE. 2008 Robust omniphobic surfaces. *Proc. Natl Acad. Sci. USA* **105**, 18 200–18 205. (doi:10.1073/pnas.0804872105)
27. Chen J *et al.* 2012 Superhydrophobic surfaces cannot reduce ice adhesion. *Appl. Phys. Lett.* **101**, 111603. (doi:10.1063/1.4752436)
28. Gent A, Lai S. 1995 Adhesion and autohesion of rubber compounds: effect of surface roughness. *Rubber Chem. Technol.* **68**, 13–25. (doi:10.5254/1.3538725)
29. Kreder MJ, Alvarenga J, Kim P, Aizenberg J. 2016 Design of anti-icing surfaces: smooth, textured or slippery? *Nat. Rev. Mater.* **1**, 15003. (doi:10.1038/natrevmats.2015.3)
30. Abe Y, Polyakov P, Skali-Lami S, Francius G. 2011 Elasticity and physico-chemical properties during drinking water biofilm formation. *Biofouling* **27**, 739–750. (doi:10.1080/08927014.2011.601300)
31. Aggarwal S, Hozalski RM. 2010 Determination of biofilm mechanical properties from tensile tests performed using a micro-cantilever method. *Biofouling* **26**, 479–486. (doi:10.1080/08927011003793080)
32. Stoodley P, Cargo R, Rupp CJ, Wilson S, Klapper I. 2002 Biofilm material properties as related to shear-induced deformation and detachment phenomena. *J. Ind. Microbiol. Biotechnol.* **29**, 361–367. (doi:10.1038/sj.jim.7000282)
33. Chaudhury MK, Finlay JA, Chung JY, Callow ME, Callow JA. 2005 The influence of elastic modulus and thickness on the release of the soft-fouling green alga Ulva linza (syn. Enteromorpha linza) from poly(dimethylsiloxane) (PDMS) model networks. *Biofouling* **21**, 41–48. (doi:10.1080/08927010500044377)
34. Berglin M, Lönn N, Gatenholm P. 2003 Coating modulus and barnacle bioadhesion. *Biofouling* **19**, 63–69. (doi:10.1080/0892701021000048774)
35. Oliveira D, Granhag L. 2016 Matching forces applied in underwater hull cleaning with adhesion strength of marine organisms. *J. Mar. Sci. Eng.* **4**, 66. (doi:10.3390/jmse4040066)

36. Sloan Jr ED, Koh C. 2007 *Clathrate hydrates of natural gases*. Boca Raton, FL: CRC Press.
37. Petrenko VF, Whitworth RW. 1999 *Physics of ice*. Oxford, UK: Oxford University Press.
38. Yirtici O, Tuncer IH, Ozgen S. 2016 Ice accretion prediction on wind turbines and consequent power losses. *J. Phys: Conf. Ser.* **753**, 022022. (doi:10.1088/1742-6596/753/2/022022)
39. Boreyko JB, Collier CP. 2013 Delayed frost growth on jumping-drop superhydrophobic surfaces. *ACS Nano* **7**, 1618–1627. (doi:10.1021/nn3055048)
40. He M, Wang J, Li H, Jin X, Wang J, Liu B, Song Y. 2010 Super-hydrophobic film retards frost formation. *Soft Matter* **6**, 2396–2399. (doi:10.1039/c0sm00024h)
41. Katz A, Alimova A, Xu M, Rudolph E, Shah MK, Savage HE, Rosen RB, McCormick SA, Alfano RR. 2003 Bacteria size determination by elastic light scattering. *IEEE J. Sel. Top. Quantum Electron.* **9**, 277–287. (doi:10.1109/JSTQE.2003.811284)
42. Mueller LN, De Brouwer JF, Almeida JS, Stal LJ, Xavier JB. 2006 Analysis of a marine phototrophic biofilm by confocal laser scanning microscopy using the new image quantification software PHLIP. *BMC Ecol.* **6**, 1. (doi:10.1186/1472-6785-6-1)
43. Barsanti L, Gualtieri, P. 2014 *Algae: anatomy, biochemistry, and biotechnology*. Boca Raton, FL CRC Press.
44. Ngan Y, Price IR. 1979 Systematic significance of spore size in the Florideophyceae (Rhodophyta). *Br. Phycol. J.* **14**, 285–303. (doi:10.1080/00071617900650311)
45. Almqvist N, Delamo Y, Smith B, Thomson N, Bartholdson Å, Lal R, Brzezinski M, Hansma P. 2001 Micromechanical and structural properties of a pennate diatom investigated by atomic force microscopy. *J. Microsc.* **202**, 518–532. (doi:10.1046/j.1365-2818.2001.00887.x)
46. Towler BF, Rebbapragada S. 2004 Mitigation of paraffin wax deposition in cretaceous crude oils of Wyoming. *J. Petrol. Sci. Eng.* **45**, 11–19. (doi:10.1016/j.petrol.2004.05.006)
47. Eberle P, Tiwari MK, Maitra T, Poulikakos D. 2014 Rational nanostructuring of surfaces for extraordinary icephobicity. *Nanoscale* **6**, 4874–4881. (doi:10.1039/C3NR06644D)
48. Heydari G, Thormann E, Jarn M, Tyrode E, Claesson PM. 2013 Hydrophobic surfaces: topography effects on wetting by supercooled water and freezing delay. *J. Phys. Chem. C* **117**, 21 752–21 762. (doi:10.1021/jp404396m)
49. Jung S, Dorrestijn M, Raps D, Das A, Megaridis CM, Poulikakos D. 2011 Are superhydrophobic surfaces best for icephobicity? *Langmuir* **27**, 3059–3066. (doi:10.1021/la104762g)
50. Chen Y, Norde W, van der Mei HC, Busscher HJ. 2012 Bacterial cell surface deformation under external loading. *MBio* **3**, e00378-12. (doi:10.1128/mBio.00378-12)
51. Wang J, Severtson SJ, Stein A. 2006 Significant and concurrent enhancement of stiffness, strength, and toughness for paraffin wax through organoclay addition. *Adv. Mater.* **18**, 1585–1588. (doi:10.1002/adma.200502615)
52. DeSain J, Brady B, Metzler K, Curtiss T, Albright T. 2009 Tensile tests of paraffin wax for hybrid rocket fuel grains. In *45th AIAA/ASME/SAE/ASEE Joint Propulsion Conf. & Exhibit*, p. 5115. August 2009, Denver, Colorado: Aerospace Research Central.
53. Tatinclaux J-C, Hirayama K-I. 1982 Determination of the flexural strength and elastic modulus of ice from in situ cantilever-beam tests. *Cold Reg. Sci. Technol.* **6**, 37–47. (doi:10.1016/0165-232X(82)90043-X)
54. Ecker C, Dvorkin J, Nur AM. 2000 Estimating the amount of gas hydrate and free gas from marine seismic data. *Geophysics* **65**, 565–573. (doi:10.1190/1.1444752)
55. Belkofsi R, Adjaoud O, Bellabbas I. 2018 Pressure induced phase transitions and elastic properties of $CaCO_3$ polymorphs: a density functional theory study. *Model. Simul. Mater. Sci. Eng.* **26**, 065004. (doi:10.1088/1361-651x/aacbed)
56. Zhang J, Reeder RJ. 1999 Comparative compressibilities of calcite-structure carbonates: deviations from empirical relations. *Am. Mineral.* **84**, 861–870. (doi:10.2138/am-1999-5-620)
57. Rykaczewski K, Anand S, Subramanyam SB, Varanasi KK. 2013 Mechanism of frost formation on lubricant-impregnated surfaces. *Langmuir* **29**, 5230–5238. (doi:10.1021/la400801s)
58. Sojoudi H, Wang M, Boscher N, McKinley G, Gleason K. 2016 Durable and scalable icephobic surfaces: similarities and distinctions from superhydrophobic surfaces. *Soft Matter* **12**, 1938–1963. (doi:10.1039/C5SM02295A)
59. Thomas SK, Cassoni RP, MacArthur CD. 1996 Aircraft anti-icing and de-icing techniques and modeling. *J. Aircraft* **33**, 841–854. (doi:10.2514/3.47027)

60. Farzaneh M, Volat C, Leblond A. 2008 Anti-icing and de-icing techniques for overhead lines. In *Atmospheric icing of power networks*, pp. 229–268. Berlin, Germany: Springer.
61. Frankenstein S, Tuthill AM. 2002 Ice adhesion to locks and dams: past work; future directions? *J. Cold Regions Eng.* **16**, 83–96. (doi:10.1061/(ASCE)0887-381X(2002)16:2(83)
62. Fillion R, Riahi A, Edrisy A. 2014 A review of icing prevention in photovoltaic devices by surface engineering. *Renew. Sustain. Energy Rev.* **32**, 797–809. (doi:10.1016/j.rser.2014.01.015)
63. Parent O, Ilinca A. 2011 Anti-icing and de-icing techniques for wind turbines: critical review. *Cold Reg. Sci. Technol.* **65**, 88–96. (doi:10.1016/j.coldregions.2010.01.005)
64. Tuteja A, Choi W, McKinley GH, Cohen RE, Rubner MF. 2008 Design parameters for superhydrophobicity and superoleophobicity. *MRS Bull.* **33**, 752–758. (doi:10.1557/mrs2008.161)
65. Cassie A, Baxter S. 1944 Wettability of porous surfaces. *Trans. Faraday Soc.* **40**, 546–551. (doi:10.1039/tf9444000546)
66. Boinovich L, Emelyanenko AM, Korolev VV, Pashinin AS. 2014 Effect of wettability on sessile drop freezing: when superhydrophobicity stimulates an extreme freezing delay. *Langmuir* **30**, 1659–1668. (doi:10.1021/la403796g)
67. Guo P, Zheng Y, Wen M, Song C, Lin Y, Jiang L. 2012 Icephobic/anti-icing properties of micro/nanostructured surfaces. *Adv. Mater.* **24**, 2642–2648. (doi:10.1002/adma.201104412)
68. He M, Wang J, Li H, Song Y. 2011 Super-hydrophobic surfaces to condensed micro-droplets at temperatures below the freezing point retard ice/frost formation. *Soft Matter* **7**, 3993–4000. (doi:10.1039/c0sm01504k)
69. Tourkine P, Le Merrer M, Quéré D. 2009 Delayed freezing on water repellent materials. *Langmuir* **25**, 7214–7216. (doi:10.1021/la900929u)
70. Bartolo D, Bouamrirene F, Verneuil E, Buguin A, Silberzan P, Moulinet S. 2006 Bouncing or sticky droplets: impalement transitions on superhydrophobic micropatterned surfaces. *EPL* **74**, 299. (doi:10.1209/epl/i2005-10522-3)
71. Bahadur V, Mishchenko L, Hatton B, Taylor JA, Aizenberg J, Krupenkin T. 2011 Predictive model for ice formation on superhydrophobic surfaces. *Langmuir* **27**, 14 143–14 150. (doi:10.1021/la200816f)
72. Kulinich S, Farhadi S, Nose K, Du X. 2010 Superhydrophobic surfaces: are they really ice-repellent? *Langmuir* **27**, 25–29. (doi:10.1021/la104277q)
73. Liu B, Lange FF. 2006 Pressure induced transition between superhydrophobic states: configuration diagrams and effect of surface feature size. *J. Colloid Interface Sci.* **298**, 899–909. (doi:10.1016/j.jcis.2006.01.025)
74. Narhe R, Beysens D. 2007 Growth dynamics of water drops on a square-pattern rough hydrophobic surface. *Langmuir* **23**, 6486–6489. (doi:10.1021/la062021y)
75. Reyssat M, Yeomans J, Quéré D. 2007 Impalement of fakir drops. *EPL* **81**, 26006. (doi:10.1209/0295-5075/81/26006)
76. Varanasi KK, Deng T, Smith JD, Hsu M, Bhate N. 2010 Frost formation and ice adhesion on superhydrophobic surfaces. *Appl. Phys. Lett.* **97**, 234102. (doi:10.1063/1.3524513)
77. Wier KA, McCarthy TJ. 2006 Condensation on ultrahydrophobic surfaces and its effect on droplet mobility: ultrahydrophobic surfaces are not always water repellant. *Langmuir* **22**, 2433–2436. (doi:10.1021/la0525877)
78. Yin L, Xia Q, Xue J, Yang S, Wang Q, Chen Q. 2010 In situ investigation of ice formation on surfaces with representative wettability. *Appl. Surf. Sci.* **256**, 6764–6769. (doi:10.1016/j.apsusc.2010.04.086)
79. Wong T-S, Kang SH, Tang SK, Smythe EJ, Hatton BD, Grinthal A, Aizenberg J. 2011 Bioinspired self-repairing slippery surfaces with pressure-stable omniphobicity. *Nature* **477**, 443. (doi:10.1038/nature10447)
80. Gwak Y, Park J-I, Kim M, Kim HS, Kwon MJ, Oh SJ, Kim Y-P, Jin E. 2015 Creating anti-icing surfaces via the direct immobilization of antifreeze proteins on aluminum. *Sci. Rep.* **5**, 12019. (doi:10.1038/srep12019)
81. Yin X, Zhang Y, Wang D, Liu Z, Liu Y, Pei X, Yu B, Zhou F. 2015 Integration of self-lubrication and near-infrared photothermogenesis for excellent anti-icing/deicing performance. *Adv. Funct. Mater.* **25**, 4237–4245. (doi:10.1002/adfm.201501101)
82. Chen J *et al.* 2013 Robust prototypical anti-icing coatings with a self-lubricating liquid water layer between ice and substrate. *ACS Appl. Mater. Interfaces* **5**, 4026–4030. (doi:10.1021/am401004t)

83. Esser-Kahn AP, Trang V, Francis MB. 2010 Incorporation of antifreeze proteins into polymer coatings using site-selective bioconjugation. *J. Am. Chem. Soc.* **132**, 13 264–13 269. (doi:10.1021/ja103038p)
84. Stone HA. 2012 Ice-phobic surfaces that are wet. *ACS Nano* **6**, 6536–6540. (doi:10.1021/nn303372q)
85. Kim P, Wong T-S, Alvarenga J, Kreder MJ, Adorno-Martinez WE, Aizenberg J. 2012 Liquid-infused nanostructured surfaces with extreme anti-ice and anti-frost performance. *ACS Nano* **6**, 6569–6577. (doi:10.1021/nn302310q)
86. Liu Q, Yang Y, Huang M, Zhou Y, Liu Y, Liang X. 2015 Durability of a lubricant-infused electrospray silicon rubber surface as an anti-icing coating. *Appl. Surf. Sci.* **346**, 68–76. (doi:10.1016/j.apsusc.2015.02.051)
87. Wilson PW, Lu W, Xu H, Kim P, Kreder MJ, Alvarenga J, Aizenberg J. 2013 Inhibition of ice nucleation by slippery liquid-infused porous surfaces (SLIPS). *Phys. Chem. Chem. Phys.* **15**, 581–585. (doi:10.1039/C2CP43586A)
88. Subramanyam SB, Rykaczewski K, Varanasi KK. 2013 Ice adhesion on lubricant-impregnated textured surfaces. *Langmuir* **29**, 13 414–13 418. (doi:10.1021/la402456c)
89. Vogel N, Belisle RA, Hatton B, Wong T-S, Aizenberg J. 2013 Transparency and damage tolerance of patternable omniphobic lubricated surfaces based on inverse colloidal monolayers. *Nat. Commun.* **4**, 2176. (doi:10.1038/ncomms3176)
90. Meuler AJ, Smith JD, Varanasi KK, Mabry JM, McKinley GH, Cohen RE. 2010 Relationships between water wettability and ice adhesion. *ACS Appl. Mater. Interfaces* **2**, 3100–3110. (doi:10.1021/am1006035)
91. Golovin K, Kobaku SP, Lee DH, DiLoreto ET, Mabry JM, Tuteja A. 2016 Designing durable icephobic surfaces. *Sci. Adv.* **2**, e1501496. (doi:10.1126/sciadv.1501496)
92. Chen J, Luo Z, Fan Q, Lv J, Wang J. 2014 Anti-ice coating inspired by ice skating. *Small* **10**, 4693–4699. (doi:10.1002/smll.201401557)
93. Dou R, Chen J, Zhang Y, Wang X, Cui D, Song Y, Jiang L, Wang J. 2014 Anti-icing coating with an aqueous lubricating layer. *ACS Appl. Mater. Interfaces* **6**, 6998–7003. (doi:10.1021/am501252u)
94. Lee H, Alcaraz ML, Rubner MF, Cohen RE. 2013 Zwitter-wettability and antifogging coatings with frost-resisting capabilities. *ACS Nano* **7**, 2172–2185. (doi:10.1021/nn3057966)
95. Sun X, Damle VG, Liu S, Rykaczewski K. 2015 Bioinspired stimuli-responsive and antifreeze-secreting anti-icing coatings. *Adv. Mater. Interfaces* **2**, 1400479. (doi:10.1002/admi.201400479)
96. Petrenko V, Peng S. 2003 Reduction of ice adhesion to metal by using self-assembling monolayers (SAMs). *Can. J. Phys.* **81**, 387–393. (doi:10.1139/p03-014)
97. Sojoudi H, McKinley GH, Gleason KK. 2015 Linker-free grafting of fluorinated polymeric cross-linked network bilayers for durable reduction of ice adhesion. *Mater. Horiz.* **2**, 91–99. (doi:10.1039/C4MH00162A)
98. Zou M, Beckford S, Wei R, Ellis C, Hatton G, Miller M. 2011 Effects of surface roughness and energy on ice adhesion strength. *Appl. Surf. Sci.* **257**, 3786–3792. (doi:10.1016/j.apsusc.2010.11.149)
99. Li X, Zhao Y, Li H, Yuan X. 2014 Preparation and icephobic properties of polymethyltrifluoropropylsiloxane–polyacrylate block copolymers. *Appl. Surf. Sci.* **316**, 222–231. (doi:10.1016/j.apsusc.2014.07.097)
100. Susoff M, Siegmann K, Pfaffenroth C, Hirayama M. 2013 Evaluation of icephobic coatings—screening of different coatings and influence of roughness. *Appl. Surf. Sci.* **282**, 870–879. (doi:10.1016/j.apsusc.2013.06.073)
101. Zhu L, Xue J, Wang Y, Chen Q, Ding J, Wang Q. 2013 Ice-phobic coatings based on silicon-oil-infused polydimethylsiloxane. *ACS Appl. Mater. Interfaces* **5**, 4053–4062. (doi:10.1021/am400704z)
102. Urata C, Dunderdale GJ, England MW, Hozumi A. 2015 Self-lubricating organogels (SLUGs) with exceptional syneresis-induced anti-sticking properties against viscous emulsions and ices. *J. Mater. Chem. A* **3**, 12 626–12 630. (doi:10.1039/C5TA02690C)
103. Wang Y, Yao X, Chen J, He Z, Liu J, Li Q, Wang J, Jiang L. 2015 Organogel as durable anti-icing coatings. *Sci. China Mater.* **58**, 559–565. (doi:10.1007/s40843-015-0069-7)
104. Makkonen L. 2012 Ice adhesion—theory, measurements and countermeasures. *J. Adhes. Sci. Technol.* **26**, 413–445.

105. Jellinek H, Kachi H, Kittaka S, Lee M, Yokota R. 1978 Ice releasing block-copolymer coatings. *Colloid Polym. Sci.* **256**, 544–551. (doi:10.1007/BF01639199)
106. Beemer DL, Wang W, Kota AK. 2016 Durable gels with ultra-low adhesion to ice. *J. Mater. Chem. A* **4**, 18 253–18 258. (doi:10.1039/C6TA07262C)
107. Wang C, Fuller T, Zhang W, Wynne KJ. 2014 Thickness dependence of ice removal stress for a polydimethylsiloxane nanocomposite: Sylgard 184. *Langmuir* **30**, 12 819–12 826. (doi:10.1021/la5030444)
108. Golovin K, Tuteja A. 2017 A predictive framework for the design and fabrication of icephobic polymers. *Sci. Adv.* **3**, e1701617. (doi:10.1126/sciadv.1701617)
109. Gbaruko B, Igwe J, Gbaruko P, Nwokeoma R. 2007 Gas hydrates and clathrates: flow assurance, environmental and economic perspectives and the Nigerian liquified natural gas project. *J. Petrol. Sci. Eng.* **56**, 192–198. (doi:10.1016/j.petrol.2005.12.011)
110. Sum AK, Koh CA, Sloan EDJI, Research EC. 2009 Clathrate hydrates: from laboratory science to engineering practice. *Ind. Eng. Chem. Res.* **48**, 7457–7465. (doi:10.1021/ie900679m)
111. Devarakonda S, Groysman A, Myerson AS. 1999 THF–water hydrate crystallization: an experimental investigation. *J. Cryst. Growth* **204**, 525–538. (doi:10.1016/S0022-0248(99)00220-1)
112. Koh C, Westacott R, Zhang W, Hirachand K, Creek J, Soper A. 2002 Mechanisms of gas hydrate formation and inhibition. *Fluid Phase Equilib.* **194**, 143–151. (doi:10.1016/S0378-3812(01)00660-4)
113. Sloan Jr ED. 2003 Fundamental principles and applications of natural gas hydrates. *Nature* **426**, 353. (doi:10.1038/nature02135)
114. Gao S. 2009 Hydrate risk management at high watercuts with anti-agglomerant hydrate inhibitors. *Energy Fuels* **23**, 2118–2121. (doi:10.1021/ef8009876)
115. Nicholas JW, Dieker LE, Sloan ED, Koh CA. 2009 Assessing the feasibility of hydrate deposition on pipeline walls—adhesion force measurements of clathrate hydrate particles on carbon steel. *J. Colloid Interface Sci.* **331**, 322–328. (doi:10.1016/j.jcis.2008.11.070)
116. Aspenes G, Dieker L, Aman Z, Høiland S, Sum A, Koh C, Sloan E. 2010 Adhesion force between cyclopentane hydrates and solid surface materials. *J. Colloid Interface Sci.* **343**, 529–536. (doi:10.1016/j.jcis.2009.11.071)
117. Smith JD, Meuler AJ, Bralower HL, Venkatesan R, Subramanian S, Cohen RE, McKinley GH, Varanasi KK. 2012 Hydrate-phobic surfaces: fundamental studies in clathrate hydrate adhesion reduction. *Phys. Chem. Chem. Phys.* **14**, 6013–6020. (doi:10.1039/c2cp40581d)
118. Sojoudi H, Walsh MR, Gleason KK, McKinley GH. 2015 Designing durable vapor-deposited surfaces for reduced hydrate adhesion. *Adv. Mater. Interfaces* **2**, 1500003. (doi:10.1002/admi.201500003)
119. Bhushan B. 2016 *Biomimetics: bioinspired hierarchical-structured surfaces for green science and technology*. Berlin, Germany: Springer.
120. Azimi G, Cui Y, Sabanska A, Varanasi KK. 2014 Scale-resistant surfaces: fundamental studies of the effect of surface energy on reducing scale formation. *Appl. Surf. Sci.* **313**, 591–599. (doi:10.1016/j.apsusc.2014.06.028)
121. Müller-Steinhagen H, Zhao Q. 1997 Investigation of low fouling surface alloys made by ion implantation technology. *Chem. Eng. Sci.* **52**, 3321–3332. (doi:10.1016/S0009-2509(97)00162-0)
122. Rankin B, Adamson W. 1973 Scale formation as related to evaporator surface conditions. *Desalination* **13**, 63–87. (doi:10.1016/S0011-9164(00)80092-2)
123. Masoudi A, Irajizad P, Farokhnia N, Kashyap V, Ghasemi H. 2017 Antiscaling magnetic slippery surfaces. *ACS Appl. Mater. Interfaces* **9**, 21 025–21 033. (doi:10.1021/acsami.7b05564)
124. Jiang W, He J, Xiao F, Yuan S, Lu H, Liang B. 2015 Preparation and antiscaling application of superhydrophobic anodized CuO nanowire surfaces. *Ind. Eng. Chem. Res.* **54**, 6874–6883. (doi:10.1021/acs.iecr.5b00444)
125. Subramanyam SB, Azimi G, Varanasi KK. 2014 Designing lubricant-impregnated textured surfaces to resist scale formation. *Adv. Mater. Interfaces* **1**, 1300068. (doi:10.1002/admi.201300068)
126. Zhao Q, Liu Y, Wang S. 2005 Surface modification of water treatment equipment for reducing $CaSO_4$ scale formation. *Desalination* **180**, 133–138. (doi:10.1016/j.desal.2005.01.002)

127. Alahmad M. 2008 Factors affecting scale formation in sea water environments—an experimental approach. *Chem. Eng. Technol.: Ind. Chem. - Plant Equip. - Process Eng. – Biotechnol.* **31**, 149–156.
128. Bornhorst A, Muller-Steinhagen H, Zhao Q. 1999 Reduction of scale formation under pool boiling conditions by ion implantation and magnetron sputtering on heat transfer surfaces. *Heat Transfer Eng.* **20**, 6–14. (doi:10.1080/014576399271529)
129. Bargir S, Dunn S, Jefferson B, Macadam J, Parsons S. 2009 The use of contact angle measurements to estimate the adhesion propensity of calcium carbonate to solid substrates in water. *Appl. Surf. Sci.* **255**, 4873–4879. (doi:10.1016/j.apsusc.2008.12.017)
130. Cheong W, Gaskell P, Neville A. 2013 Substrate effect on surface adhesion/crystallisation of calcium carbonate. *J. Cryst. Growth* **363**, 7–21. (doi:10.1016/j.jcrysgro.2012.09.025)
131. Zhao Q, Wang X. 2005 Heat transfer surfaces coated with fluorinated diamond-like carbon films to minimize scale formation. *Surf. Coat. Technol.* **192**, 77–80. (doi:10.1016/j.surfcoat.2004.02.030)
132. Vazirian MM, Charpentier TV, de Oliveira Penna M, Neville A. 2016 Surface inorganic scale formation in oil and gas industry: as adhesion and deposition processes. *J. Petrol. Sci. Eng.* **137**, 22–32. (doi:10.1016/j.petrol.2015.11.005)
133. Zettler H, Wei M, Zhao Q, Müller-Steinhagen H. 2005 Influence of surface properties and characteristics on fouling in plate heat exchangers. *Heat Transfer Eng.* **26**, 3–17. (doi:10.1080/01457630590897024)
134. Förster M, Bohnet M. 2000 Modification of molecular interactions at the interface crystal/heat transfer surface to minimize heat exchanger fouling. *Int. J. Therm. Sci.* **39**, 697–708. (doi:10.1016/S1290-0729(00)00229-5)
135. Herz A, Malayeri M, Müller-Steinhagen H. 2008 Fouling of roughened stainless steel surfaces during convective heat transfer to aqueous solutions. *Energy Convers. Manage.* **49**, 3381–3386. (doi:10.1016/j.enconman.2007.09.034)
136. Keysar S, Semiat R, Hasson D, Yahalom J. 1994 Effect of surface roughness on the morphology of calcite crystallizing on mild steel. *J. Colloid Interface Sci.* **162**, 311–319. (doi:10.1006/jcis.1994.1044)
137. Müller-Steinhagen H, Zhao Q, Helali-Zadeh A, Ren XG. 2000 The effect of surface properties on $CaSO_4$ scale formation during convective heat transfer and subcooled flow boiling. *Can. J. Chem. Eng.* **78**, 12–20. (doi:10.1002/cjce.5450780105)
138. Elminir HK, Ghitas AE, Hamid R, El-Hussainy F, Beheary M, Abdel-Moneim KM. 2006 Effect of dust on the transparent cover of solar collectors. *Energy Convers. Manage.* **47**, 3192–3203. (doi:10.1016/j.enconman.2006.02.014)
139. Jang GG, Smith DB, List FA, Lee DF, Ievlev AV, Collins L, Park J, Polizos G. 2018 The anti-soiling performance of highly reflective superhydrophobic nanoparticle-textured mirrors. *Nanoscale* **10**, 14 600–14 612. (doi:10.1039/C8NR03024C)
140. Ju F, Fu X. 2011 Research on impact of dust on solar photovoltaic (PV) performance. In *2011 Int. Conf. on Electrical and Control Engineering (ICECE)*, pp. 3601–3606, IEEE.
141. Said SA, Al-Aqeeli N, Walwil HM. 2015 The potential of using textured and anti-reflective coated glasses in minimizing dust fouling. *Sol. Energy* **113**, 295–302. (doi:10.1016/j.solener.2015.01.007)
142. Said SA, Walwil HM. 2014 Fundamental studies on dust fouling effects on PV module performance. *Sol. Energy* **107**, 328–337. (doi:10.1016/j.solener.2014.05.048)
143. Sarver T, Al-Qaraghuli A, Kazmerski LL. 2013 A comprehensive review of the impact of dust on the use of solar energy: History, investigations, results, literature, and mitigation approaches. *Renew. Sustain. Energy Rev.* **22**, 698–733. (doi:10.1016/j.rser.2012.12.065)
144. Corn M. 1961 The adhesion of solid particles to solid surfaces. I. A review. *J. Air Pollut. Contr. Assoc.* **11**, 523–528. (doi:10.1080/00022470.1961.10468032)
145. Bell IH, Groll EA. 2011 Air-side particulate fouling of microchannel heat exchangers: experimental comparison of air-side pressure drop and heat transfer with plate-fin heat exchanger. *Appl. Therm. Eng.* **31**, 742–749. (doi:10.1016/j.applthermaleng.2010.10.019)
146. Bott T, Bemrose C. 1983 Particulate fouling on the gas-side of finned tube heat exchangers. *J. Heat Transfer* **105**, 178–183. (doi:10.1115/1.3245538)

147. Dove A, Devaud G, Wang X, Crowder M, Lawitzke A, Haley C. 2011 Mitigation of lunar dust adhesion by surface modification. *Planet. Space Sci.* **59**, 1784–1790. (doi:10.1016/j.pss.2010.12.001)
148. Sabri F, Werhner T, Hoskins J, Schuerger A, Hobbs A, Barreto J, Britt D, Duran R. 2008 Thin film surface treatments for lowering dust adhesion on Mars Rover calibration targets. *Adv. Space Res.* **41**, 118–128. (doi:10.1016/j.asr.2007.06.074)
149. Stubbs TJ, Vondrak RR, Farrell WM. 2007 Impact of dust on lunar exploration. See http://hefd.jsc.nasa.gov/files/StubbsImpactOnExploration.
150. He G, Zhou C, Li Z. 2011 Review of self-cleaning method for solar cell array. *Procedia Eng.* **16**, 640–645. (doi:10.1016/j.proeng.2011.08.1135)
151. Liu K, Jiang L. 2012 Bio-inspired self-cleaning surfaces. *Annu. Rev. Mater. Res.* **42**, 231–263. (doi:10.1146/annurev-matsci-070511-155046)
152. Ragesh P, Ganesh VA, Nair SV, Nair AS. 2014 A review on 'self-cleaning and multifunctional materials'. *J. Mater. Chem. A* **2**, 14 773–14 797. (doi:10.1039/C4TA02542C)
153. Cuddihy EF. 1980 Theoretical considerations of soil retention. *Solar Energy Mater.* **3**, 21–33. (doi:10.1016/0165-1633(80)90047-7)
154. Bowling RA. 1985 An analysis of particle adhesion on semiconductor surfaces. *J. Electrochem. Soc.* **132**, 2208–2214. (doi:10.1149/1.2114320)
155. Joseph S, Ytzhaki T, Kasis E, Sheinman A, Yadin, I. 2016 Transparent dust repellent coating for sapphire. In *Optical interference coatings*, p. TB. 10. Optical Society of America.
156. Sueto T, Ota Y, Nishioka K. 2013 Suppression of dust adhesion on a concentrator photovoltaic module using an anti-soiling photocatalytic coating. *Sol. Energy* **97**, 414–417. (doi:10.1016/j.solener.2013.09.006)
157. Quan Y-Y, Zhang L-Z. 2017 Experimental investigation of the anti-dust effect of transparent hydrophobic coatings applied for solar cell covering glass. *Sol. Energy Mater. Sol. Cells* **160**, 382–389. (doi:10.1016/j.solmat.2016.10.043)
158. Crowder MS, Haley C. 2008 Mitigating molecular and particulate contamination via surface energy. In *Optical system contamination: effects, measurements, and control, San Diego, California, USA, 2 September 2008*. p. 706909. Washington, USA: International Society for Optics and Photonics.
159. Sanjay M, Simanta B, Kulwant S. 1995 Paraffin problems in crude oil production and transportation: a review. *SPE Prod. Facil.* **10**, 50–54. (doi:10.2118/28181-PA)
160. Kelechukwu EM, Al-Salim HS, Saadi A. 2013 Prediction of wax deposition problems of hydrocarbon production system. *J. Petrol. Sci. Eng.* **108**, 128–136. (doi:10.1016/j.petrol.2012.11.008)
161. Al-Yaari M. 2011 Paraffin wax deposition: mitigation and removal techniques. In SPE Saudi Arabia Section Young Professionals Technical Symposium. Society of Petroleum Engineers.
162. Wang J, Buckley JS, Creek JL. 2004 Asphaltene deposition on metallic surfaces. *J. Dispersion Sci. Technol.* **25**, 287–298. (doi:10.1081/DIS-120037697)
163. Patil AO, Zushma S, Berluche E, Varma-Nair M. 2002 Wax crystal modifiers (LAW657). (Google Patents).
164. Pedersen KS, Rønningsen HP. 2003 Influence of wax inhibitors on wax appearance temperature, pour point, and viscosity of waxy crude oils. *Energy Fuels* **17**, 321–328. (doi:10.1021/ef020142+)
165. Kraiwattanawong K, Fogler HS, Gharfeh SG, Singh P, Thomason WH, Chavadej S. 2009 Effect of asphaltene dispersants on aggregate size distribution and growth. *Energy Fuels* **23**, 1575–1582. (doi:10.1021/ef800706c)
166. Etoumi A. 2007 Microbial treatment of waxy crude oils for mitigation of wax precipitation. *J. Petrol. Sci. Eng.* **55**, 111–121. (doi:10.1016/j.petrol.2006.04.015)
167. Brown F. 1992 Microbes: The practical and environmental safe solution to production problems, enhanced production, and enhanced oil recovery. In Permian Basin Oil and Gas Recovery Conf. Society of Petroleum Engineers.
168. Jorda R. 1966 Paraffin deposition and prevention in oil wells. *J. Petrol. Technol.* **18**, 605–601, 612. (doi:10.2118/1598-PA)
169. Zholondz IA, Finkelstein MI. 1962 Lakokrasochnye Materialy i Ikh Primenenie pp. 40–44.
170. Paso K, Kompalla T, Aske N, Rønningsen HP, Øye G, Sjöblom J. 2009 Novel surfaces with applicability for preventing wax deposition: a review. *J. Dispersion Sci. Technol.* **30**, 757–781. (doi:10.1080/01932690802643220)

171. Zaitseva TA, Gonik AA, Maksheyev Y, Permyakov NG. 1968 *Trudy, Ufimskii Neftyanoi Nauchno-Issledovatel'skii Institut*, pp. 141–144.
172. Patton CC, Casad BM. 1970 Paraffin deposition from refined wax-solvent systems. *Soc. Petrol. Eng. J.* **10**, 17–24. (doi:10.2118/2503-PA)
173. Jun T, Qunji X. 1998 Effect on the wettability between doating and liquid paraffin by the dispersion component and polar component of coating surface energy. *Chem. Eng. Oil Gas* **2**, 018.
174. Quintella CM, Musse APS, Castro MT, Scaiano J, Mikelsons L, Watanabe YN. 2006 Polymeric surfaces for heavy oil pipelines to inhibit wax deposition: PP, EVA28, and HDPE. *Energy Fuels* **20**, 620–624. (doi:10.1021/ef050267p)
175. Zhang X, Tian J, Wang L, Zhou Z. 2002 Wettability effect of coatings on drag reduction and paraffin deposition prevention in oil. *J. Petrol. Sci. Eng.* **36**, 87–95. (doi:10.1016/S0920-4105(02)00267-X)
176. Rashidi M, Mombekov B, Marhamati M. 2016 A study of a novel inter pipe coating material for paraffin wax deposition control and comparison of the results with current mitigation technique in oil and gas industry. In *Offshore Technology Conf. Asia (Offshore Technology Conf.)*.
177. Dotto M, Martins R, Ferreira M, Camargo Jr S. 2006 Influence of hydrogenated amorphous carbon coatings on the formation of paraffin deposits. *Surf. Coat. Technol.* **200**, 6479–6483. (doi:10.1016/j.surfcoat.2005.11.061)
178. Bixler GD, Bhushan B. 2012 Biofouling: lessons from nature. *Phil. Trans. R. Soc. A* **370**, 2381–2417. (doi:10.1098/rsta.2011.0502)
179. Engelsman AF, Saldarriaga-Fernandez IC, Nejadnik MR, van Dam GM, Francis KP, Ploeg RJ, Busscher HJ, van der Mei HC. 2010 The risk of biomaterial-associated infection after revision surgery due to an experimental primary implant infection. *Biofouling* **26**, 761–767. (doi:10.1080/08927014.2010.515027)
180. Ward WK. 2008 *A review of the foreign-body response to subcutaneously-implanted devices: the role of macrophages and cytokines in biofouling and fibrosis*. Beverley Hills, CA: SAGE Publications.
181. Wisniewski N, Reichert M. 2000 Methods for reducing biosensor membrane biofouling. *Colloids Surf. B: Biointerfaces* **18**, 197–219. (doi:10.1016/S0927-7765(99)00148-4)
182. Edmiston CE, Seabrook GR, Goheen MP, Krepel CJ, Johnson CP, Lewis BD, Brown KR, Towne JB. 2006 Bacterial adherence to surgical sutures: can antibacterial-coated sutures reduce the risk of microbial contamination? *J. Am. Coll. Surg.* **203**, 481–489. (doi:10.1016/j.jamcollsurg.2006.06.026)
183. Kluge RM, Calia FM, McLaughlin JS, Hornick RB. 1974 Sources of contamination in open heart surgery. *J.Am. Med. Assoc.* **230**, 1415–1418. (doi:10.1001/jama.1974.03240100033023)
184. Schmalzried TP, Amstutz HC, Au M-K, Dorey FJ. 1992 Etiology of deep sepsis in total hip arthroplasty. The significance of hematogenous and recurrent infections. *Clin. Orthopaed. Relat. Res.* **280**, 200–207. (doi:10.1097/00003086-199207000-00026)
185. Chan J, Wong S. 2010 *Biofouling: types, impact and anti-fouling*. New York, NY: Nova Science Publishers, Incorporated.
186. Chopra V, O'horo JC, Rogers MA, Maki DG, Safdar N. 2013 The risk of bloodstream infection associated with peripherally inserted central catheters compared with central venous catheters in adults: a systematic review and meta-analysis. *Infect. Control Hosp. Epidemiol.* **34**, 908–918. (doi:10.1086/671737)
187. Maki DG, Tambyah PA. 2001 Engineering out the risk for infection with urinary catheters. *Emerg. Infect. Dis.* **7**, 342. (doi:10.3201/eid0702.010240)
188. Peters G, Locci R, Pulverer G. 1982 Adherence and growth of coagulase-negative Staphylococci on surfaces of intravenous catheters. *Emerg. Infect. Dis.* **146**, 479–482. (doi:10.1093/infdis/146.4.479)
189. Attaway III HH, Fairey S, Steed LL, Salgado CD, Michels HT, Schmidt MG. 2012 Intrinsic bacterial burden associated with intensive care unit hospital beds: effects of disinfection on population recovery and mitigation of potential infection risk. *Am. J. Infect. Control* **40**, 907–912. (doi:10.1016/j.ajic.2011.11.019)
190. Appendini P, Hotchkiss JH. 2002 Review of antimicrobial food packaging. *Innov. Food Sci. Emerg. Technol.* **3**, 113–126. (doi:10.1016/S1466-8564(02)00012-7)

191. Han JH. 2003 Antimicrobial food packaging. In *Novel food packaging techniques*, vol. 8 (ed. R Ahvenainen), pp. 50–70. Boca Raton, FL: CRC Press.
192. Petersen K, Nielsen PV, Bertelsen G, Lawther M, Olsen MB, Nilsson NH, Mortensen G. 1999 Potential of biobased materials for food packaging. *Trends Food Sci. Technol.* **10**, 52–68. (doi:10.1016/S0924-2244(99)00019-9)
193. Quintavalla S, Vicini L. 2002 Antimicrobial food packaging in meat industry. *Meat Sci.* **62**, 373–380. (doi:10.1016/S0309-1740(02)00121-3)
194. Flemming H-C. 1997 Reverse osmosis membrane biofouling. *Exp. Therm. Fluid Sci.* **14**, 382–391. (doi:10.1016/S0894-1777(96)00140-9)
195. Hyun J, Jang H, Kim K, Na K, Tak T. 2006 Restriction of biofouling in membrane filtration using a brush-like polymer containing oligoethylene glycol side chains. *J. Membr. Sci.* **282**, 52–59. (doi:10.1016/j.memsci.2006.05.008)
196. Lee W, Ahn CH, Hong S, Kim S, Lee S, Baek Y, Yoon J. 2010 Evaluation of surface properties of reverse osmosis membranes on the initial biofouling stages under no filtration condition. *J. Membr. Sci.* **351**, 112–122. (doi:10.1016/j.memsci.2010.01.035)
197. Mansouri J, Harrisson S, Chen V. 2010 Strategies for controlling biofouling in membrane filtration systems: challenges and opportunities. *J. Mater. Chem.* **20**, 4567–4586. (doi:10.1039/b926440j)
198. Potts D, Ahlert RC, Wang SS. 1981 A critical review of fouling of reverse osmosis membranes. *Desalination* **36**, 235–264. (doi:10.1016/S0011-9164(00)88642-7)
199. Hellio C, Yebra D. 2009 *Advances in marine antifouling coatings and technologies*. Cambridge, UK: Woodhead Publishing.
200. Townsin R. 2003 The ship hull fouling penalty. *Biofouling* **19**, 9–15. (doi:10.1080/0892701031000088535)
201. Edyvean R, Terry L, Picken G. 1985 Marine fouling and its effects on offshore structures in the North Sea: a review. *Int. Biodeterior.* **21**, 277–284.
202. Houghton D. 1978 Marine fouling and offshore structures. *Ocean Manage.* **4**, 347–352. (doi:10.1016/0302-184X(78)90033-1)
203. Magin CM, Cooper SP, Brennan AB. 2010 Non-toxic antifouling strategies. *Mater. Today* **13**, 36–44. (doi:10.1016/S1369-7021(10)70058-4)
204. Chambers LD, Stokes KR, Walsh FC, Wood RJ. 2006 Modern approaches to marine antifouling coatings. *Surface Coat. Technol.* **201**, 3642–3652. (doi:10.1016/j.surfcoat.2006.08.129)
205. Wahl M. 1989 Marine epibiosis. I. Fouling and antifouling: some basic aspects. *Mar. Ecol. Prog. Ser.* **58**, 175–189. (doi:10.3354/meps058175)
206. Hucknall A, Rangarajan S, Chilkoti A. 2009 In pursuit of zero: polymer brushes that resist the adsorption of proteins. *Adv. Mater.* **21**, 2441–2446. (doi:10.1002/adma.200900383)
207. Banerjee I, Pangule RC, Kane RS. 2011 Antifouling coatings: recent developments in the design of surfaces that prevent fouling by proteins, bacteria, and marine organisms. *Adv. Mater.* **23**, 690–718. (doi:10.1002/adma.201001215)
208. Zhang H, Chiao M. 2015 Anti-fouling coatings of poly (dimethylsiloxane) devices for biological and biomedical applications. *J. Med. Biol. Eng.* **35**, 143–155. (doi:10.1007/s40846-015-0029-4)
209. Amiji M, Park K. 1992 Prevention of protein adsorption and platelet adhesion on surfaces by PEO/PPO/PEO triblock copolymers. *Biomaterials* **13**, 682–692. (doi:10.1016/0142-9612(92)90128-B)
210. Gong P, Grainger DW. 2007 Nonfouling surfaces. In *Microarrays* pp. 59–92. Berlin, Germany: Springer.
211. Ji B, Gao H. 2004 Mechanical properties of nanostructure of biological materials. *J. Mech. Phys. Solids* **52**, 1963–1990. (doi:10.1016/j.jmps.2004.03.006)
212. Gosline J, Lillie M, Carrington E, Guerette P, Ortlepp C, Savage K. 2002 Elastic proteins: biological roles and mechanical properties. *Phil. Trans. R. Soc. Lond. B* **357**, 121–132. (doi:10.1098/rstb.2001.1022)
213. Jeon S, Lee J, Andrade J, De Gennes P, Science I. 1991 Protein–surface interactions in the presence of polyethylene oxide: I. Simplified theory. *J. Colloid Interface Sci.* **142**, 149–158. (doi:10.1016/0021-9797(91)90043-8)

214. Prime KL, Whitesides GM. 1991 Self-assembled organic monolayers: model systems for studying adsorption of proteins at surfaces. *Science* **252**, 1164–1167. (doi:10.1126/science.252.5009.1164)
215. Bearinger J, Terrettaz S, Michel R, Tirelli N, Vogel H, Textor M, Hubbell J. 2003 Chemisorbed poly (propylene sulphide)-based copolymers resist biomolecular interactions. *Nat. Mater.* **2**, 259. (doi:10.1038/nmat851)
216. Mrksich M, Whitesides GM. 1996 Using self-assembled monolayers to understand the interactions of man-made surfaces with proteins and cells. *Annu. Rev. Biophys. Biomol. Struct.* **25**, 55–78. (doi:10.1146/annurev.bb.25.060196.000415)
217. Li L, Chen S, Zheng J, Ratner BD, Jiang S. 2005 Protein adsorption on oligo (ethylene glycol)-terminated alkanethiolate self-assembled monolayers: the molecular basis for nonfouling behavior. *J. Phys. Chem. B* **109**, 2934–2941. (doi:10.1021/jp0473321)
218. Andrade J, Hlady V, Wei A, Ho C, Lea A, Jeon S, Lin Y, Stroup E. 1992 Proteins at interfaces: principles, multivariate aspects, protein resistant surfaces, and direct imaging and manipulation of adsorbed proteins. In *Biologically modified polymeric biomaterial surfaces*, pp. 67–84. Berlin, Germany: Springer.
219. Jeon S, Andrade J. 1991 Protein—surface interactions in the presence of polyethylene oxide: II. Effect of protein size. *J. Colloid Interface Sci.* **142**, 159–166. (doi:10.1016/0021-9797(91)90044-9)
220. Jeon S, Andrade J. 1991 Protein—surface interactions in the presence of polyethylene oxide: II. Effect of protein size. *J. Colloid Interface Sci.* **142**, 149–158.
221. Sofia SJ, Premnath V, Merrill EW. 1998 Poly (ethylene oxide) grafted to silicon surfaces: grafting density and protein adsorption. *Macromolecules* **31**, 5059–5070. (doi:10.1021/ma971016l)
222. Norde W. 2003 Driving forces for protein adsorption at solid surfaces. In *Biopolymers at interfaces*, vol. 110 (ed. M Malmsten). New York, NY: Marcel Dekker.
223. Prime KL, Whitesides GM. 1993 Adsorption of proteins onto surfaces containing end-attached oligo (ethylene oxide): a model system using self-assembled monolayers. *J. Am. Chem. Soc.* **115**, 10 714–10 721. (doi:10.1021/ja00076a032)
224. Tegoulia VA, Rao W, Kalambur AT, Rabolt JF, Cooper SL. 2001 Surface properties, fibrinogen adsorption, and cellular interactions of a novel phosphorylcholine-containing self-assembled monolayer on gold. *Langmuir* **17**, 4396–4404. (doi:10.1021/la001790t)
225. He Y, Hower J, Chen S, Bernards MT, Chang Y, Jiang S. 2008 Molecular simulation studies of protein interactions with zwitterionic phosphorylcholine self-assembled monolayers in the presence of water. *Langmuir* **24**, 10 358–10 364. (doi:10.1021/la8013046)
226. Keefe AJ, Jiang S. 2012 Poly (zwitterionic) protein conjugates offer increased stability without sacrificing binding affinity or bioactivity. *Nat. Chem.* **4**, 59. (doi:10.1038/nchem.1213)
227. Chang Y, Liao S-C, Higuchi A, Ruaan R-C, Chu C-W, Chen W-Y. 2008 A highly stable nonbiofouling surface with well-packed grafted zwitterionic polysulfobetaine for plasma protein repulsion. *Langmuir* **24**, 5453–5458. (doi:10.1021/la800228c)
228. Laughlin RG. 1991 Fundamentals of the zwitterionic hydrophilic group. *Langmuir* **7**, 842–847. (doi:10.1021/la00053a006)
229. Schlenoff JB. 2014 Zwitteration: coating surfaces with zwitterionic functionality to reduce nonspecific adsorption. *Langmuir* **30**, 9625–9636. (doi:10.1021/la500057j)
230. Hsiao S-W, Venault A, Yang H-S, Chang Y. 2014 Bacterial resistance of self-assembled surfaces using PPOm-b-PSBMAn zwitterionic copolymer–concomitant effects of surface topography and surface chemistry on attachment of live bacteria. *Colloids Surf. B: Biointerfaces* **118**, 254–260. (doi:10.1016/j.colsurfb.2014.03.051)
231. Mi L, Jiang S. 2014 Integrated antimicrobial and nonfouling zwitterionic polymers. *Angew. Chem. Int. Ed.* **53**, 1746–1754. (doi:10.1002/anie.201304060)
232. Li G, Cheng G, Xue H, Chen S, Zhang F, Jiang S. 2008 Ultra low fouling zwitterionic polymers with a biomimetic adhesive group. *Biomaterials* **29**, 4592–4597. (doi:10.1016/j.biomaterials.2008.08.021)
233. Zhao W, Ye Q, Hu H, Wang X, Zhou F. 2014 Grafting zwitterionic polymer brushes via electrochemical surface-initiated atomic-transfer radical polymerization for anti-fouling applications. *J. Biomed. Mater. Res. B Appl. Biomater.* **2**, 5352–5357.

234. Chen S *et al.* 2016 Durable antibacterial and nonfouling cotton textiles with enhanced comfort via zwitterionic sulfopropylbetaine coating. *Small* **12**, 3516–3521. (doi:10.1002/smll.201600587)
235. Nguyen AT, Baggerman J, Paulusse JM, van Rijn CJ, Zuilhof H. 2011 Stable protein-repellent zwitterionic polymer brushes grafted from silicon nitride. *Langmuir* 223, 2587–2594. (doi:10.1021/la104657c)
236. Yeh S-B, Chen C-S, Chen W-Y, Huang C-J. 2014 Modification of silicone elastomer with zwitterionic silane for durable antifouling properties. *Langmuir* **30**, 11 386–11 393. (doi:10.1021/la502486e)
237. Jiang H, Wang X, Li C, Li J, Xu F, Mao C, Yang W, Shen J. 2011 Improvement of hemocompatibility of polycaprolactone film surfaces with zwitterionic polymer brushes. *Langmuir* **27**, 11 575–11 581. (doi:10.1021/la202101q)
238. Qin G, Cai C. 2009 Oxidative degradation of oligo (ethylene glycol)-terminated monolayers. *Chem. Commun.* **34**, 5112–5114. (doi:10.1039/b911155g)
239. Saikhwan P, Chew JY, Paterson WR, Wilson DI. 2007 Swelling and its suppression in the cleaning of polymer fouling layers. *Ind. Eng. Chem. Res.* **228**, 4846–4855. (doi:10.1021/ie0615943)
240. Metzger U, Le-Clech P, Stuetz RM, Frimmel FH, Chen V. 2007 Characterisation of polymeric fouling in membrane bioreactors and the effect of different filtration modes. *J. Membr. Sci.* **301**, 180–189. (doi:10.1016/j.memsci.2007.06.016)
241. Watkinson AP. 1992 Chemical reaction fouling of organic fluids. *Chem. Eng. Technol.: Ind. Chem. -Plant Equip. -Process Eng. -Biotechnol.* **15**, 82–90.
242. Callow ME, Callow JA. 2002 Marine biofouling: a sticky problem. *Biologist* **49**, 1–5.
243. Wang Z, Pujari SP, van Lagen B, Smulders MM, Zuilhof H. 2016 Highly polymer-repellent yet atomically flat surfaces based on organic monolayers with a single fluorine atom. *Adv. Mater. Interfaces* **3**, 1500514. (doi:10.1002/admi.201500514)
244. Smol JP,Stoermer EF. 2010 *The diatoms: applications for the environmental and earth sciences*. Cambridge, UK: Cambridge University Press.
245. Losic D, Mitchell JG, Voelcker NH. 2009 Diatomaceous lessons in nanotechnology and advanced materials. *Adv. Mater.* **21**, 2947–2958. (doi:10.1002/adma.200803778)
246. Ibrahim WM, Ali RM, Hemida KA, Sayed MA. 2014 Role of Ulva lactuca extract in alleviation of salinity stress on wheat seedlings. *Sci. World J.* 2014.
247. Schultz MP. 2007 Effects of coating roughness and biofouling on ship resistance and powering. *Biofouling* **23**, 331–341. (doi:10.1080/08927010701461974)
248. Schultz MP, Kavanagh CJ, Swain GW. 1999 Hydrodynamic forces on barnacles: implications on detachment from fouling-release surfaces. *Biofouling* **13**, 323–335. (doi:10.1080/08927019909378388)
249. Jain A, Bhosle NB. 2009 Biochemical composition of the marine conditioning film: implications for bacterial adhesion. *Biofouling* **25**, 13–19. (doi:10.1080/08927010802411969)
250. Cooksey K, Wigglesworth-Cooksey B. 1995 Adhesion of bacteria and diatoms to surfaces in the sea: a review. *Aquat. Microb. Ecol.* **9**, 87–96. (doi:10.3354/ame009087)
251. Fletcher RL, Callow ME. 1992 The settlement, attachment and establishment of marine algal spores. *Br. Phycol. J.* **27**, 303–329. (doi:10.1080/00071619200650281)
252. Hellio C, De La Broise D, Dufosse L, Le Gal Y, Bourgougnon N. 2001 Inhibition of marine bacteria by extracts of macroalgae: potential use for environmentally friendly antifouling paints. *Mar. Environ. Res.* **52**, 231–247. (doi:10.1016/S0141-1136(01)00092-7)
253. Picioreanu C, Van Loosdrecht MC, Heijnen JJ. 2001 Two-dimensional model of biofilm detachment caused by internal stress from liquid flow. *Biotechnol. Bioeng.* **72**, 205–218. (doi:10.1002/1097-0290(20000120)72:2<205::AID-BIT9>3.0.CO;2-L)
254. Pavlovsky L, Younger JG, Solomon MJ. 2013 In situ rheology of Staphylococcus epidermidis bacterial biofilms. *Soft Matter* **9**, 122–131. (doi:10.1039/C2SM27005F)
255. Baier RE. 1970 Surface properties influencing biological adhesion. In *Adhesion in biological systems*, pp. 15–48. New York, NY: Academic Press.
256. Ista LK, Callow ME, Finlay JA, Coleman SE, Nolasco AC, Simons RH, Callow JA, Lopez GP. 2004 Effect of substratum surface chemistry and surface energy on attachment of marine bacteria and algal spores. *Appl. Environ. Microbiol.* **70**, 4151–4157. (doi:10.1128/AEM.70.7.4151-4157.2004)

257. Baier RE. 2006 Surface behaviour of biomaterials: the theta surface for biocompatibility. *J. Mater. Sci.: Mater. Med.* **17**, 1057. (doi:10.1007/s10856-006-0444-8)
258. Ciriminna R, Bright FV, Pagliaro M. 2015 Ecofriendly antifouling marine coatings. *ACS Sustain. Chem. Eng.* **3**, 559–565. (doi:10.1021/sc500845n)
259. Bressy C, Lejars M. 2014 Marine fouling: an overview. *J. Ocean Technol.* **9**, 19–28.
260. Thorlaksen P, Yebra DM, Catala P. 2010 Hydrogel-based third generation fouling release coatings.
261. Higaki Y, Nishida J, Takenaka A, Yoshimatsu R, Kobayashi M, Takahara A. 2015 Versatile inhibition of marine organism settlement by zwitterionic polymer brushes. *Polym. J.* **47**, 811. (doi:10.1038/pj.2015.77)
262. Zhang Z, Finlay JA, Wang L, Gao Y, Callow JA, Callow ME, Jiang S. 2009 Polysulfobetaine-grafted surfaces as environmentally benign ultralow fouling marine coatings. *Langmuir* **25**, 13 516–13 521. (doi:10.1021/la901957k)
263. Callow JA, Callow ME. 2011 Trends in the development of environmentally friendly fouling-resistant marine coatings. *Nat. Commun.* **2**, 244. (doi:10.1038/ncomms1251)
264. Peter Thorlaksen DMY, Catala P. 2013 Hydrogel based third generation fouling release coatings. World Patent WO 2013000479.
265. Ozkan A, Berberoglu H. 2013 Adhesion of algal cells to surfaces. *Biofouling* **29**, 469–482. (doi:10.1080/08927014.2013.782397)
266. Krishnan S *et al.* 2006 Anti-biofouling properties of comblike block copolymers with amphiphilic side chains. *Langmuir* **22**, 5075–5086. (doi:10.1021/la052978l)
267. Bakker DP, Huijs FM, de Vries J, Klijnstra JW, Busscher HJ, van der Mei HC. 2003 Bacterial deposition to fluoridated and non-fluoridated polyurethane coatings with different elastic modulus and surface tension in a parallel plate and a stagnation point flow chamber. *Colloids Surf., B* **32**, 179–190. (doi:10.1016/S0927-7765(03)00159-0)
268. Bakker DP, Busscher HJ, van Zanten J, de Vries J, Klijnstra JW, van der Mei HC. 2004 Multiple linear regression analysis of bacterial deposition to polyurethane coatings after conditioning film formation in the marine environment. *Microbiology* **150**, 1779–1784. (doi:10.1099/mic.0.26983-0)
269. Guégan C, Garderes J, Le Pennec G, Gaillard F, Fay F, Linossier I, Herry J-M, Fontaine M-NB, Réhel KV. 2014 Alteration of bacterial adhesion induced by the substrate stiffness. *Colloids Surf. B* **114**, 193–200. (doi:10.1016/j.colsurfb.2013.10.010)
270. Kolewe KW, Zhu J, Mako NR, Nonnenmann SS, Schiffman JD. 2018 Bacterial adhesion is affected by the thickness and stiffness of poly (ethylene glycol) hydrogels. *ACS Appl. Mater. Interfaces* **10**, 2275–2281. (doi:10.1021/acsami.7b12145)
271. Zargiel KA, Coogan JS, Swain GW. 2011 Diatom community structure on commercially available ship hull coatings. *Biofouling* **27**, 955–965. (doi:10.1080/08927014.2011.618268)
272. Francius G, Tesson B, Dague E, Martin-Jézéquel V, Dufrêne YF. 2008 Nanostructure and nanomechanics of live Phaeodactylum tricornutum morphotypes. *Environ. Microbiol.* **10**, 1344–1356. (doi:10.1111/j.1462-2920.2007.01551.x)
273. Higgins MJ, Molino P, Mulvaney P, Wetherbee R. 2003 The structure and nanomechanical properties of the adhesive mucilage that mediates diatom-substratum adhesion and motility 1. *J. Phycol.* **39**, 1181–1193. (doi:10.1111/j.0022-3646.2003.03-027.x)
274. Losic D, Short K, Mitchell JG, Lal R, Voelcker NH. 2007 AFM nanoindentations of diatom biosilica surfaces. *Langmuir* **23**, 5014–5021. (doi:10.1021/la062666y)
275. Anderson C, Atlar M, Callow M, Candries M, Milne A, Townsin R. 2003 The development of foul-release coatings for seagoing vessels. *Proc. Inst. Mar. Eng., Sci. Technol. Part B, J. Mar. Des. Oper.* **2003**, 11–23.
276. Higgins MJ, Sader JE, Mulvaney P, Wetherbee R. 2003 Probing the surface of living diatoms with atomic force microscopy: the nanostructure and nanomechanical properties of the mucilage layer 1. *J. Phycol.* **39**, 722–734. (doi:10.1046/j.1529-8817.2003.02163.x)
277. Litchman E, Klausmeier C, Yoshiyama K. 2009 Contrasting size evolution in marine and freshwater diatoms. *Proc. Natl Acad. Sci. USA* **106**, 2665–2670 (doi:10.1073/pnas.0810891106)
278. Martinelli E *et al.* 2008 Nanostructured films of amphiphilic fluorinated block copolymers for fouling release application. *Langmuir* **24**, 13 138–13 147. (doi:10.1021/la801991k)
279. Weinman CJ *et al.* 2009 ABC triblock surface active block copolymer with grafted ethoxylated fluoroalkyl amphiphilic side chains for marine antifouling/fouling-release applications. *Langmuir* **25**, 12 266–12 274. (doi:10.1021/la901654q)

280. van Zoelen W *et al.* 2014 Sequence of hydrophobic and hydrophilic residues in amphiphilic polymer coatings affects surface structure and marine antifouling/fouling release properties. *ACS Macro Lett.* **3**, 364–368. (doi:10.1021/mz500090n)
281. Gudipati CS, Finlay JA, Callow JA, Callow ME, Wooley KL. 2005 The antifouling and fouling-release performance of hyperbranched fluoropolymer (HBFP)− poly (ethylene glycol)(PEG) composite coatings evaluated by adsorption of biomacromolecules and the green fouling alga Ulva. *Langmuir* **21**, 3044–3053. (doi:10.1021/la048015o)
282. Feng S, Wang Q, Gao Y, Huang Y, Qing FL. 2009 Synthesis and characterization of a novel amphiphilic copolymer capable as anti-biofouling coating material. *J. Appl. Polym. Sci.* **114**, 2071–2078. (doi:10.1002/app.30779)
283. Hempel. See http://www.hempel.com/en/products/hempaguard-x7--89900.
284. Jacobson AH, Willingham GL. 2000 Sea-nine antifoulant: an environmentally acceptable alternative to organotin antifoulants. *Sci. Total Environ.* **258**, 103–110. (doi:10.1016/S0048-9697(00)00511-8)
285. Cima F, Bragadin M, Ballarin L. 2008 Toxic effects of new antifouling compounds on tunicate haemocytes: I. Sea-Nine 211™ and chlorothalonil. *Aquat. Toxicol.* **86**, 299–312. (doi:10.1016/j.aquatox.2007.11.010)
286. Lee H, Scherer NF, Messersmith PB. 2006 Single-molecule mechanics of mussel adhesion. *Proc. Natl Acad. Sci. USA* **103**, 12 999–13 003. (doi:10.1073/pnas.0605552103)
287. Sun Y, Guo S, Walker GC, Kavanagh CJ, Swain GW. 2004 Surface elastic modulus of barnacle adhesive and release characteristics from silicone surfaces. *Biofouling* **20**, 279–289. (doi:10.1080/08927010400026383)
288. Wynne K, Swain G, Fox R, Bullock S, Uilk J. 2000 Two silicone nontoxic fouling release coatings: hydrosilation cured PDMS and CaCO3 filled, ethoxysiloxane cured RTV11. *Biofouling* **16**, 277–288. (doi:10.1080/08927010009378451)
289. Kaffashi A, Jannesari A, Ranjbar Z. 2012 Silicone fouling-release coatings: effects of the molecular weight of poly(dimethylsiloxane) and tetraethyl orthosilicate on the magnitude of pseudobarnacle adhesion strength. *Biofouling* **28**, 729–741. (doi:10.1080/08927014.2012.702342)
290. Schultz M, Finlay J, Callow M, Callow J. 2003 Three models to relate detachment of low form fouling at laboratory and ship scale. *Biofouling* **19**, 17–26. (doi:10.1080/0892701031000089516)